Geochimica et Cosmochimica Acta, Vol. 68, No. 23, pp. 4915–4933, 2004

0016-7037/04 $30.00 + .00

doi:10.1016/j.gca.2004.05.037

# Chemistry of springs across the Mariana forearc shows progressive devolatilization of the subducting plate

MICHAEL J. MOTTL,[1,*] C. GEOFFREY WHEAT,[2] PATRICIA FRYER,[3] JIM GHARIB,[4] and JONATHAN B. MARTIN[5]

[1]Department of Oceanography, University of Hawaii, Honolulu, HI 96822, USA
[2]Global Undersea Research Unit, P.O. Box 757220, University of Alaska, Fairbanks, AK 99775, USA
[3]Hawaii Institute of Geophysics and Planetology, University of Hawaii, Honolulu, HI 96822, USA
[4]Department of Geology and Geophysics, University of Hawaii, Honolulu, HI 96822, USA
[5]Department of Geological Sciences, University of Florida, Gainesville, FL 32611, USA

(*Received July* 16, 2003; *accepted in revised form May* 17, 2004)

**Abstract**—Cold springs upwelling through large serpentinite mud volcanoes in the outer half of the Mariana forearc provide a unique window into processes of devolatilization of the subducting Pacific Plate. We have sampled upwelling pore waters with lower chlorinity than seawater from six sites on five serpentinite mud volcanoes, by conventional gravity and piston coring, by push coring from the ROV *Jason,* by drilling on ODP Legs 125 and 195, and by manned submersible. The sites range from 13°47′N to 19°33′N and 52 to 90 km from the Mariana trench axis, corresponding to approximate depths to the top of the downgoing plate of 16 to 29 km. The composition of the springs varies systematically over this distance: nearer the trench the upwelling waters have much higher Ca and Sr than seawater and much lower carbonate alkalinity, sulfate, Na/Cl, K, Rb, and B. Farther from the trench the waters show the opposite trends relative to seawater. Chlorinity is consistently lower than in seawater and shows large variations that are not systematic with distance from the trench. Cs is consistently higher than in seawater and increases with distance from the trench. All of the waters have high pH and are heavily depleted in Mg, Si, Li, F, and $^{87}Sr/^{86}Sr$ relative to seawater. They tend to be enriched in $O^{18}/O^{16}$. Except for ODP drilling, none of the cores was long enough to produce an asymptotic compositional trend with depth. We have inferred the end-member compositions of the upwelling waters by extrapolation against Mg. At two sites we were able to compare data from gravity cores with data from drill cores or push cores collected at springs to estimate the effects of reactions that occur at shallow depth below the seafloor, on mixing of the upwelling waters with seawater. These effects are different for sites high in dissolved Ca, nearer the trench, vs. those high in alkalinity, farther from the trench. Common to both are large losses from solution of 1) Ca, as $CaCO_3$ and in exchange for Na; 2) Mg, in exchange for Na or Ca and as brucite; 3) sulfate, probably reduced by microbes or possibly precipitated as gypsum; 4) Sr, Ba, Si, and F. Na is consistently leached from the solids into solution, whereas K and $O^{18}/O^{16}$ are relatively unreactive.

We infer that the upwelling waters are uniformly saturated with $CaCO_3$ and that the excess $H_2O$ and the trends in Ca, Sr, alkalinity, and sulfate with distance from the trench result from introduction of $H_2O$ and dissolved carbonate and sulfate from an external source, the sediment and altered basalt at the top of the subducting plate. The concurrent trends in Na/Cl, B, Cs, and especially K and Rb indicate that these species originate from the top of the subducting plate in response to increasing temperature. These systematic variations across the outer forearc imply that the solutions ascend more or less vertically from the source region and do not travel long distances laterally along the décollement before ascending. Based on leaching of K, the 150°C isotherm is crossed approximately beneath Big Blue Seamount at a depth of ~22 km below the seafloor, 70 km behind the trench. By this point it appears that carbonate dissolution has joined dehydration as a significant process at the top of the subducting plate. 

## 1. INTRODUCTION

As one lithospheric plate descends beneath another in a subduction zone, its upper surface experiences progressively higher pressures and temperatures, initiating a series of physical processes and chemical reactions that recrystallize the solids and drive volatile components from the downgoing slab into the mantle and crust of the overriding plate. These processes begin with sediment compaction and dehydration beneath the forearc and progress through the arc and backarc into the deeper mantle. The reactants include sediments and their contained pore water, altered basalt and gabbro of the oceanic crust, and possibly hydrated, serpentinized mantle in the subducting plate. The products include fault-controlled springs in the forearc, serpentinite in the mantle of the overriding plate, magmatism in the arc and backarc, and recrystallized rock throughout, including characteristically in the blueschist as well as greenschist and amphibolite facies. The entire process has been referred to as the "Subduction Factory" (MARGINS, 1998), in which subducted materials either make their way back to the surface or are carried deep into the mantle. A major goal of subduction zone studies is to quantify fluxes in the subduction factory. A complete understanding of subduction zones processes would require as well knowledge of pressure-temperature paths, reactions along those paths, and the kinetics of those reactions.

The output flux from subduction zones that is best charac-

* Author to whom correspondence should be addressed (mmottl@soest.hawaii.edu).

Table 1. Sites cored for this study.

| No. of cores[a] Seamount, site | Tried | Recovered | | Ranges in: | |
|---|---|---|---|---|---|
| | | Pore water | Serpentinite | North latitude | East longitude |
| Pacman | | | | | |
| Baseball Mitt | | | | 19°10.4–11.3′ | 147°2.1–4.4′ |
| Gravity cores | 20 | 15 | 15 | | |
| Piston core | 1 | 1 | 1 | 19°10.515′ | 147°2.798′ |
| Push cores[b] | 5 | 5 | 2 | 19°10.645–666′ | 147°3.597–649′ |
| Sub-Summit | 1 | 1 | 1 | 19°14.7′ | 146°55.7′ |
| East Grabens | 2 | 2 | 0 | 19°11.3, 18.3′ | 147°14.6, 8.5′ |
| Mudlumps | 4 | 3 | 0 | 19°21.6–26.1 | 146°47.6–51.9′ |
| Blue Moon | 6[c] | 5[c] | 2[c] | 15°43.1–47.5′ | 147°10.6–18.7′ |
| Big Blue | 7 | 5 | 7 | 18°5.5–7.7′ | 147°5.2–6.9′ |
| South Chamorro | 9 | 4 | 9 | 13°46.0–47.0′ | 146°0.1–0.2′ |
| NE Chamorro | 2 | 2 | 2 | 13°55.8–56.5′ | 146°14.5–15.3′ |
| NW Chamorro | 3 | 0 | 0 | 14°2.1–3.8′ | 146°2.5–2.9′ |
| Peacock | 4 | 3 | 1 | 16°1.4–2.5′ | 147°6.7–7.9′ |
| Turquoise | 1 | 1 | 1 | 16°57.065′ | 147°13.0238′ |
| Celestial | 1 | 1 | 1 | 16°32.25′ | 147°13.25′ |
| Total | 66 | 48 | 42 | | |

[a] All cores are gravity cores unless otherwise specified.
[b] From the site within the Baseball Mitt known as Cerulean Springs (Fryer et al., 1999).
[c] One of these was a piston core; the rest are gravity cores.

terized is that in the volcanic arc. It has long been known that there is an apparent imbalance between the flux of volatile material into subduction zones and that which comes out as arc magmas. Peacock (1990) estimated that on a global scale only ~16% of the $H_2O$ and 3% of the $CO_2$ delivered to the trench can be accounted for in the arc magmatic output, dissolved in arc magmas. The rest of the $H_2O$ and $CO_2$ is either released under the forearc, incorporated into the mantle of the overriding plate, lost as exsolved magmatic gases, stored in subcrustal intrusions, or returned to the deep mantle. None of these processes has been adequately quantified for any subduction zone, despite their obvious importance for the geochemical cycles of $H_2O$, $CO_2$, and other volatile species.

Two types of subduction zones can be distinguished: accretionary, in which sediment scraped off the downgoing plate accumulates landward of the trench, and nonaccretionary, in which most or all sediment delivered to the trench by the downgoing plate is subducted (Uyeda, 1982). Both types are known to have forearc springs that deliver water to the seafloor that is typically fresher than seawater (Mottl, 1992). The low chlorinity of these waters suggests that they are produced not just by expulsion of pore water during sediment compaction but also by dehydration of subducted solids. The Mariana forearc is the type example of a nonaccretionary forearc (Uyeda, 1982). It provides a unique window into processes of devolatilization of the subducting slab in the form of upwelling water and springs on serpentinite mud volcanoes in the outer half of the forearc (Fryer et al., 1990, 1999). Because the matrix protolith is depleted mantle harzburgite that is chemically simpler than typical crustal rocks and sediments, a deep slab-derived component in the upwelling water can be recognized more readily than at accretionary margins, where a thick prism of sediment is present and is likely to be a major reactant. That upwelling pore water in accretionary prisms is fresher than seawater, for example, has been attributed to dehydration of clay minerals in the accretionary sediment, membrane ultrafiltration through clays, dissolution of gas hydrates, presence of freshwater aquifers, and dehydration of the subducting plate. None of the first four processes is likely to be important in a nonaccretionary setting such as the Mariana forearc, where the upwelling low-salinity water almost certainly originates by dehydration of the downgoing plate.

In 1997 we sampled nine serpentinite mud volcanoes in the Mariana forearc using a combination of conventional gravity and piston coring, and push coring from the ROV *Jason* (Table 1). We document here a systematic variation in the composition of upwelling water across the Mariana forearc that appears to be related to progressive devolatilization of the subducting lithospheric plate, including loss of $H_2O$, $CO_2$, and other volatile species that allow us to estimate temperature at the source.

## 2. PREVIOUS WORK

Large serpentinite seamounts, up to 50 km across and 2 km high, were discovered in the Mariana forearc by Fryer et al. (1985, 1995, 2000). They are abundant in the outer forearc in a band from ~30 to 100 km behind the trench axis (Fig. 1). These mud volcanoes are believed to form when water generated by dehydration of the subducting Pacific Plate ascends into the overlying mantle of the Philippine Plate, composed mainly of depleted harzburgite, and converts it to serpentinite. This low-density rock then rises buoyantly along fractures and extrudes at the seafloor, usually as a point source, producing a mud volcano with a central conduit that is narrow relative to the diameter of the volcano. This conduit feeds flows of unconsolidated sedimentary serpentinite that comprise the bulk of the seamount. The serpentinite consists mainly of clay- and silt-sized particles of lizardite, chrysotile, and brucite. Suspended within this fine-grained matrix and supported by it are variably serpentinized clasts of harzburgite ranging in size from silt to large boulders, along with typically a few percent of metamorphosed mafic clasts (e.g., Fryer and Mottl, 1992; Johnson,

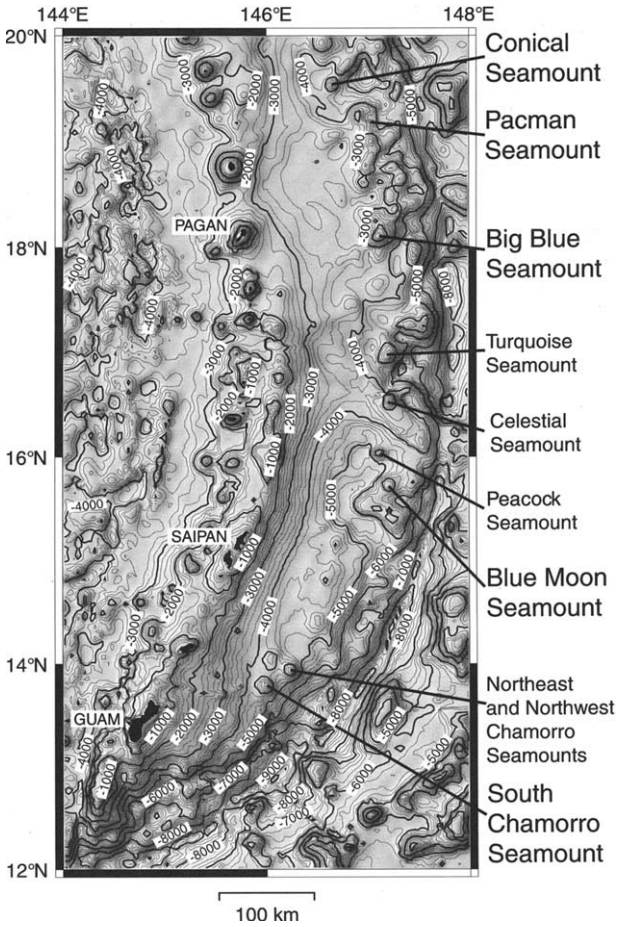


Fig. 1. Bathymetry of the Mariana forearc showing the locations of ten serpentinite mud volcanoes where pore waters have been sampled.

1992; Shipboard Scientific Party, 2002). Bulk chemical analyses of harzburgite clasts and serpentinite mud from ODP Sites 778 to 780 on Conical Seamount and ODP Site 1200 on South Chamorro Seamount summit are given in Table 2. On both seamounts the depleted harzburgite protolith comprises ~80% magnesian (Fo 92%) olivine and 20% orthopyroxene with only 0 to 2% each of clinopyroxene and chromian spinel (Ishii et al., 1992; Parkinson et al., 1992; Shipboard Scientific Party, 2002).

Cold springs were first observed on these seamounts in 1987 from the manned submersible *Alvin,* near the summit of Conical Seamount, 90 km arcward (west) of the trench axis at 19°33′N (Fryer et al., 1990). These springs had formed chimneys up to 3.5 m high composed of aragonite, calcite, and amorphous Mg-silicate, which were lightly covered by bacterial mats and small limpets and gastropods. When one chimney was disturbed by sampling it began to emit a slow flow of cold water, near the 1.5°C temperature of the ambient bottom water, with pH 9.3 and elevated alkalinity, methane, sulfate, and reduced sulfur relative to the ambient seawater (Fryer et al., 1990). Low-salinity pore water upwelling through serpentinite mud at the summit of Conical Seamount was sampled at Ocean Drilling Program (ODP) Site 780 in 1989 (Fryer et al., 1992). It had less than half the chloride and bromide content of seawater and pH as high as 12.6. Relative to seawater it had higher to much higher sulfate, dissolved carbonate, light hydrocarbons, ammonia, Na/Cl, K, Rb, B, $\delta^{18}O$, and $\delta D$; and lower to much lower Mg, Ca, Sr, Li, Si, phosphate, and Sr isotopic ratio (Mottl, 1992; Mottl et al., 2003; Table 3). Dissolved sulfide of 2 mmol/kg was measured in one sample from 3 m below the seafloor (mbsf). Near-surface gradients in chloride indicate that this water was upwelling at seepage velocities of 1 to 10 cm/yr relative to the serpentinite matrix (Mottl, 1992). How fast the matrix is upwelling is unknown, but it must be fast enough to keep large boulders of harzburgite in suspension despite the inherent weakness of the mud (Shipboard Scientific Party, 1990, p. 167; Phipps and Ballotti, 1992). Although the springs on Conical Seamount summit were cold, a temperature of 13.5°C was measured at a depth of 58 mbsf by logging of the open Hole 780C following drilling, vs. only 3.7°C extrapolated for the same depth from discrete measurements made while drilling the adjacent Hole 780D. The higher temperature in the open borehole implies that drilling induced upward flow of warm water in Hole 780C (Shipboard Scientific Party, 1990; Mottl, 1992).

Also drilled on Leg 125 was Torishima Forearc Seamount, an inactive serpentinite mud volcano at 31°56′N in the Izu-Bonin forearc. Pore water recovered from serpentinite on this seamount reflects reaction of cool (4 to 11°C) seawater with harzburgite and contrasts greatly with that from the active Conical Seamount: it shows the opposite direction of change relative to seawater for chloride, sulfate, dissolved carbonate, K, Rb, Ca, Sr, B, $\delta^{18}O$, and $\delta D$; its Na/Cl is unchanged; and its pH, methane, Si, and ammonia are not nearly as high (Mottl, 1992; Mottl et al., 2003). The distinctive composition of water upwelling at Conical Seamount (Table 3) implies that it originates by dehydration of the subducting Pacific plate, ~29 km below the seafloor at this site based on earthquake depths (Hussong and Fryer, 1981; Seno and Maruyama, 1984). The upwelling $H_2O$ is in excess of that which hydrates the mantle wedge during its ascent, and represents an early return of subducted volatiles through the forearc to the oceans.

Springs were discovered on the summit of another serpentinite mud volcano, South Chamorro Seamount, 85 km arcward of the trench at 13°47′N, in 1996 (Fryer and Mottl, 1997). Divers in the manned submersible *Shinkai-6500* (Dive 351) found three cold springs that were populated by an abundant biota of mussels, small tubeworms, whelks, and galatheid crabs. Carbonate crusts and small chimneys up to 0.3 m high were also found, although no venting of water could be seen. Three push cores were collected at the springs that yielded pore water reflective of their composition (Table 3). A series of holes was drilled near one of these springs as ODP Site 1200 in 2001 (Shipboard Scientific Party, 2002). Except for its higher chlorinity, which was 94% of that in ambient bottom seawater, the upwelling pore water recovered from serpentinite on South Chamorro Seamount is remarkably similar to that from Conical Seamount and is upwelling at a similar speed (Mottl et al., 2003; Table 3). Depth profiles of pore-water composition clarified the cause of the high dissolved sulfide found earlier at shallow depth at Conical Seamount: as documented at South Chamorro Seamount, a microbial community dominated overwhelmingly by *Archaea* is oxidizing methane and reducing sulfate from the deep upwelling water as well as from seawater, at pH 12.5, producing measured concentrations of dissolved

Table 2. Composition of harzburgite clasts and serpentinite mud from two mud volcanoes in the Mariana forearc.

| | Conical Seamount | | | | S. Chamorro Seamount | |
|---|---|---|---|---|---|---|
| | Harzburgite clasts[a] | | Serpentinite mud[b] | | Harzburgite clasts[c] | |
| wt% | Average | SD ± 1σ | Average | SD ± 1σ | Average | SD ± 1σ |
| $SiO_2$ | 40.29 | 0.98 | 38.91 | 1.71 | 37.87 | 0.51 |
| $TiO_2$ | 0.00 | 0.00 | 0.02 | 0.06 | 0.01 | 0.00 |
| $Al_2O_3$ | 0.67 | 0.12 | 0.74 | 0.29 | 0.56 | 0.14 |
| $Fe_2O_{3T}$ | 8.03 | 0.55 | 6.84 | 0.40 | 7.18 | 0.30 |
| MnO | 0.10 | 0.01 | 0.11 | 0.03 | 0.10 | 0.00 |
| MgO | 40.42 | 1.53 | 38.09 | 1.20 | 40.50 | 0.55 |
| CaO | 0.57 | 0.33 | 0.39 | 0.28 | 0.68 | 0.25 |
| $Na_2O$ | 0.00 | 0.00 | 0.22 | 0.10 | 0.08 | 0.04 |
| $K_2O$ | 0.00 | 0.00 | 0.02 | 0.03 | 0.02 | 0.01 |
| $P_2O_5$ | 0.00 | 0.00 | 0.03 | 0.02 | 0.03 | 0.02 |
| LOI | 8.23 | 2.49 | 14.30 | 1.16 | 13.50 | 1.69 |
| Total | 98.32 | | 99.66 | | 100.52 | |
| $CaCO_3$ | | | 0.92[d] | 0.59 | | |
| $C_{org}$ | | | 0.20[d] | 0.09 | | |
| S | | | 0.03[d] | 0.06 | | |
| ppm: | | | | | | |
| Li | | | 3.6 | 5.6 | | |
| Rb | 0.2 | 0.1 | 2 | 0 | | |
| Sr | 3.3 | 3.7 | 12 | 10 | 21 | 9 |
| Ba | | | 15 | 0 | 7 | 3 |
| V | 36 | 7 | 17 | 3 | 26 | 8 |
| Cr | 2459 | 281 | 1808 | 742 | 2746 | 390 |
| Co | 115 | 4 | 89 | 18 | | |
| Ni | 2327 | 286 | 1934 | 408 | 2591 | 232 |
| Cu | 7 | 4 | 25 | 11 | | |
| Zn | 39 | 3 | 38 | 9 | | |

[a] Average of five samples from Holes 778A, 779A, and 780C, from Parkinson et al. (1992) and Ishii et al. (1992). Clasts are 54 ± 26% serpentinized (range 20–85%).

[b] Average of 10 samples from Hole 778A, from Lagabrielle et al. (1992). Samples with high content of clay (Al >3.2%) or $CaCO_3$ (Ca >1%) have been excluded.

[c] Average of 20 samples from Holes 1200A and 1200B, from Shipboard Scientific Party (2002). Clasts are 70 ± 19% serpentinized (range 37–100%).

[d] Average of 45 samples from Sites 778, 779, and 780, from Shipboard Scientific Party (1990). S was undetectable (<0.01 wt %) in 31 of 45 samples. For muds from Site 1200 on S. Chamorro Seamount, values are 0.81 ± 0.36 wt % $CaCO_3$, 0.01 ± 0.02 wt % $C_{org}$, and 0.01 ± 0.007 wt % S, except in a near-surface zone of C and S enrichment, which has been excluded here.

sulfide as high as 20 mmol/kg. This extremophilic microbial community presumably provides the sustenance for the macrobiota found at the South Chamorro springs.

In 1997 we sampled nine serpentinite mud volcanoes in the Mariana forearc using a combination of gravity coring, piston coring, and push coring from the ROV *Jason* (Table 1). Our preliminary results were reported by Fryer et al. (1999). Here we present a detailed analysis of the composition of pore waters obtained from these cores and use these data to infer systematic changes in the composition of fluids driven off the top of the subducting Pacific Plate as it descends beneath the Philippine Plate at the Mariana convergent margin. These changes allow us further to estimate temperature at the top of the downgoing plate.

## 3. METHODS

Cores were split and sampled immediately after arrival onboard ship. Samples of serpentinite mud and any overlying pelagic sediment were cooled to 1° to 4°C and centrifuged to separate pore water, which was filtered through 0.45 μm nylon filters and analyzed onboard for pH (±0.01 1σ) by ion-specific electrode, alkalinity (±2%) by potentiometric Gran titration with 0.1 N HCl, chlorinity (±0.2%) by automated electrochemical titration with silver nitrate, Ca (±0.5%) by automated electrochemical titration with EGTA, and Mg (±0.2%) by colorimetric titration for total alkaline earths with EDTA, using IAPSO seawater as a standard. Appropriately acidified or unacidified aliquots were stored in acid-cleaned high-density polyethylene bottles and analyzed onshore for sulfate (±2%) by ion chromatography; K (±2%) by flame atomic absorption spectrophotometry; Li (±1%) and Rb (±4%) by flame emission spectrophotometry using standard additions; Sr, Ba, Mn, Fe, Si, and B (±4%) by inductively-coupled plasma (ICP) atomic emission spectrometry; Cs (±3%) by ICP-mass spectrometry; F (±2%) by ion-specific electrode with correction for Mg concentration; and $\delta^{18}O$ (±0.1‰) (stored in sealed glass ampules) and $^{87}Sr/^{86}Sr$ (±0.00002) by mass spectrometry. Na (±0.3%) was calculated from charge balance by difference. Total dissolved hydroxyl-bearing species and carbonate alkalinity were calculated from the above chemical analyses using the computer program PHREEQC (Parkhurst and Appelo, 1999) to determine the distribution of aqueous species at 2.4°C.

## 4. RESULTS

For this study we attempted 66 cores at 12 sites on nine serpentinite mud volcanoes (Table 1). Forty-eight of these cores recovered pore water and 42 recovered serpentinite; six coring

Table 3. Composition of ascending pore water at six sites with distance from the Mariana Trench.[a]

| | Bottom seawater | Pacman[b] BB Mitt | Blue Moon summit | Pacman summit | Big Blue summit | S. Chamorro S351 spring[c] | Seamount Site 1200 | Conical Site 780 |
|---|---|---|---|---|---|---|---|---|
| North latitude | | 19°10.66′ | 15°43.1′ | 19°14.7′ | 18°7.0′ | 13°47.0′ | 13°47.0′ | 19°32.5′ |
| East longitude | | 147°3.63′ | 147°10.6′ | 146°55.7′ | 147°5.8′ | 146°0.2′ | 146°0.2′ | 146°39.2′ |
| No. of samples | | 15 | 12–36 | 6 | 7–21 | 7 | 53 | 15 |
| Deepest sample (mbsf) | | 0.22 | 4.04 | 1.04 | 1.28 | 0.23 | 71 | 130 |
| Distance from trench (km) | | 52 | 55 | 64 | 70 | 85 | 85 | 90 |
| Slab depth (km)[d] | | 16 | 17 | 20 | 22 | 27 | 27 | 29 |
| pH (*assumed) | 8 | 12.5* | 12.5* | 12.5* | 12.5* | 11.42 | 12.5 | 12.5 |
| | mEq/kg: | | | | | | | |
| Alkalinity | 2.3 | 13 | 13 | 13 | 13 | **18.4** | **62** | **52** |
| Carb. sp. | 2.3 | 0 | 0 | 0 | 0 | **14.0** | **46** | **35** |
| $OH^-$ sp. | 0 | 13 | 13 | 13 | 13 | 1.2 | 13 | 13 |
| | mmol/kg: | | | | | | | |
| Chlorinity | 542 | 386 | 512 | 419 | 538 | 518 | 510 | 260 |
| Sulfate | 28 | 12.3 | 0.01 | 19.0 | 9.7 | 27.1 | **28** | **46** |
| Mg | 52.4 | 0 | 0 | 0 | 0 | <0.01 | <0.01 | 0.003 |
| Ca | 10.2 | **51.2** | **52.0** | 0 | 0 | 0.03 | 0.3 | 1 |
| Na | 466 | 314 | 414 | 465 | 560 | 570 | 610 | 390 |
| Na/Cl | 0.86 | 0.82 | 0.81 | **1.11** | **1.04** | **1.10** | **1.20** | **1.50** |
| K | 10.1 | 6.3 | 4.2 | 6.5 | **12.8** | **16.3** | **19** | **15** |
| | μmol/kg: | | | | | | | |
| Li | 26 | 10.0 | 2.5 | na | 15.4 | 0.02 | 0.4 | 1.6 |
| Rb | 1.37 | 1.2 | 0.3 | **1.8** | **2.6** | **8.8** | **10** | **7.8** |
| Cs | 0.002 | **0.011** | **0.016** | **0.038** | **0.032** | **0.35** | **0.36** | **0.15** |
| Sr | 90 | **325** | **1008** | 33 | 0 | 14.4 | 10 | 20 |
| Ba | 0.14 | **0.63** | **0.53** | **0.26** | 0.05 | 0.14 | **0.4** | 0.1 |
| B | 410 | 87 | 370 | **890** | **1250** | **3259** | **3200** | **3900** |
| Si | 190 | 68 | 0 | 0 | 0 | 24 | 70 | 60 |
| F | 67 | 0 | 0 | 0 | 0 | 81 | 47 | na |
| Mn | 0 | 0.06 | 0.02 | 0 | 0.08 | 0.01 | 0.01 | <0.01 |
| Fe | 0 | 0.18 | 5.8 | 0 | 0 | 0.0 | 2 | 2 |
| $\delta^{18}O$ (o/oo SMOW)[e] | 0 | >0.52 | −0.67 | −0.09 | −0.22 | na | 2.5 | 4.0 |
| $^{87}Sr/^{86}Sr$[f] | 0.7091 | 0.70265 | na | na | 0.709 | 0.70627 | 0.70535 | <0.7062 |
| Min. T (°C), for 1% shear[g] | | 102 | 106 | 120 | 128 | | 149 | 157 |
| Max. T (°C), for 5% shear[g] | | 137 | 145 | 170 | 187 | | 231 | 249 |

[a] Compositions were determined by extrapolating to Mg = −6.5 mmol/kg, to account for precipitation of brucite on mixing, except for S. Chamorro and Conical, where data are from Fryer and Mottl (1997) and Mottl et al. (2003). Some values are shown in bold to emphasize that they are greater than in seawater.

[b] Pacman Baseball Mitt composition is based on push cores collected by ROV *Jason* at Cerulean Springs.

[c] S351 spring is that sampled on *Shinkai-6500* Dive 351 in November 1996 (Fryer and Mottl, 1997).

[d] Depth to the top of the subducting slab is estimated from earthquake depths (Hussong and Fryer, 1981; Seno and Maruyama, 1984).

[e] Oxygen isotopic data are from Benton (1997), Mottl et al. (2003), and J. Martin (this study).

[f] Strontium isotopic data are from Haggerty and Chaudhuri (1992), Mottl et al. (2003), and J. Martin (this study).

[g] Minimum and maximum temperature estimates are for shear stress of 1% and 5% of lithostatic pressure, from Figure 11.

attempts recovered only rocks and one only sand, five had too little sediment to yield pore water, and six came up empty. Only eight cores recovered serpentinite exclusively, of which four also yielded pore water; these eight cores are all from the summits of Big Blue and South Chamorro Seamounts. Besides serpentinite most of the cores recovered as well an overlying layer of hemipelagic, foraminifera- and volcanic ash–rich sediment; this layer is absent only where serpentinite has protruded or flowed recently. The longest gravity core was 2.5 m (average 1.1 m), the longer of two piston cores was 4.1 m, and the longest of five push cores collected by the *Jason* ROV was 23 cm.

Five of nine seamounts yielded pore water that was similar to bottom seawater, indicating either that these seamounts do not harbor deep upwelling waters or, more likely, that we failed to core a sufficiently active spot to detect such upwelling in the short cores we obtained. Two of the four sites on Pacman Seamount, one comprising several small (100 m high) mudlumps and the other a pair of grabens, likewise yielded essentially seawater. Sites that showed no evidence for upwelling of deep slab-derived fluids will not be discussed further here, although we intend to revisit them in the future to look again for such evidence. We focus instead on the five sites on four seamounts that did show such evidence and compare them in Table 3 with the well-characterized deep water from Conical Seamount, ODP Site 780, and South Chamorro Seamount, ODP Site 1200 (Mottl et al., 2003).

### 4.1. Composition of the Upwelling Water

The five sites we cored that showed evidence for active upwelling of deeply sourced water are the Baseball Mitt and

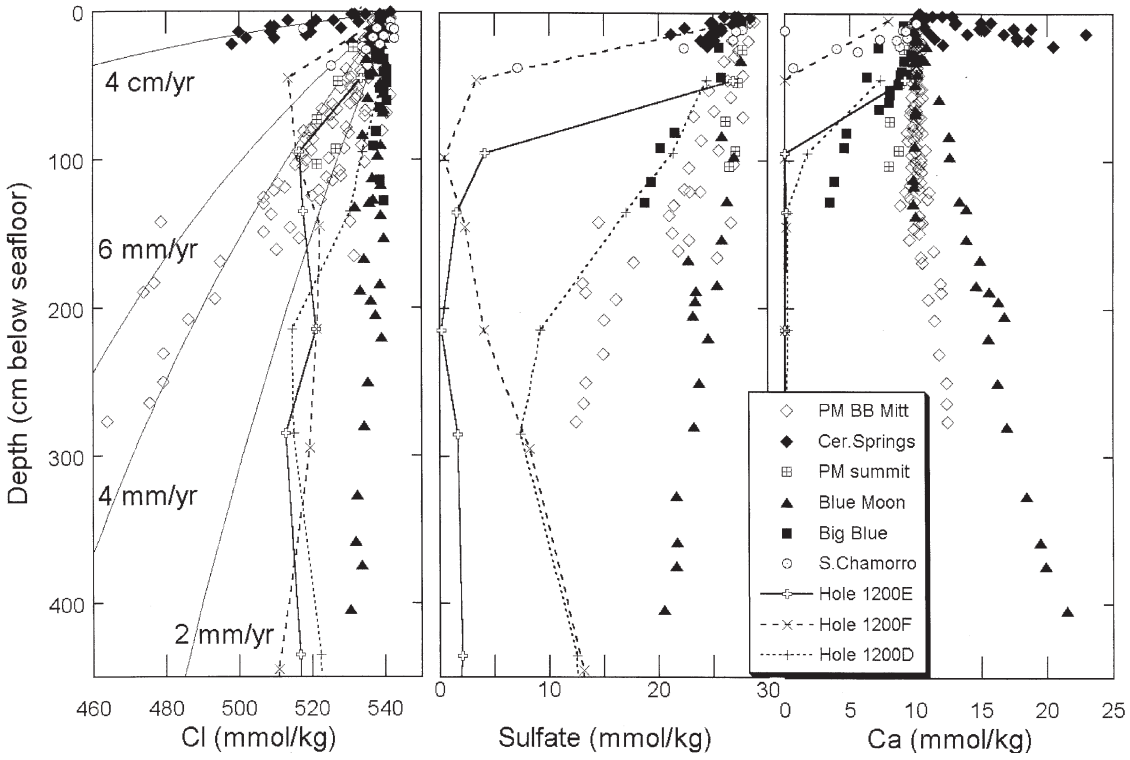


Fig. 2. Chlorinity, sulfate, and Ca in pore waters from four Mariana forearc serpentinite mud volcanoes. Cerulean Springs are located within the Baseball Mitt site on Pacman (PM) Seamount and were sampled by *Jason* push cores; other Baseball (BB) Mitt data are from gravity and piston cores. Upwelling (seepage) speeds are calculated for a Baseball Mitt pore water with 386 mmol/kg chlorinity (Table 3) at 2°C, porosity 0.57, formation factor 3, $D_w$ for Cl 0.0336, and $D_{sed}$ 0.0196 $m^2$/yr. South Chamorro data are from gravity cores, push cores collected from *Shinkai-6500,* and drill cores from ODP Site 1200.

eastern subsummit on Pacman Seamount and the summits of Blue Moon, Big Blue, and South Chamorro Seamounts. The Baseball Mitt, a region of high backscatter shaped in map view like a baseball mitt (see fig. 4 in Fryer and Fryer, 1987), lies on the southeastern flank of Pacman Seamount. These sites range in distance from the axis of the Mariana Trench from 52 to 90 km (Table 3). The chlorinity of interstitial water and the concentrations of dissolved sulfate and Ca at these five sites are plotted against depth in Figure 2, along with similar data from three ODP drillholes at Site 1200 on the summit of South Chamorro Seamount. Two sets of data from the Baseball Mitt are distinguished in Figure 2: push cores collected by the ROV *Jason* and gravity and piston cores collected by conventional means from the R/V *Thompson*. The push cores were taken at a site of active venting, as indicated by presence of 10-cm high chimneys composed of brucite and called Cerulean Springs by Fryer et al. (1999). They display much higher chemical gradients than do the gravity and piston cores. None of these cores penetrated deeply enough to produce the convex-upward depth profiles and asymptotic concentrations characteristic of upwelling of pore water that differs in composition from seawater. Nevertheless, the higher chemical gradients in the push cores are consistent with a much higher upwelling (seepage) speed closer to the Cerulean Springs, in the range of 2 to 6 cm/yr (Fig. 2), and strongly suggest that the gradients in general are produced mainly by upwelling rather than by diffusion alone, in agreement with the earlier conclusion of Fryer et al. (1999). Away from Cerulean Springs upwelling in the Baseball Mitt is much slower, ~0.1 to 0.8 cm/yr when uncertainty in the formation factor (which is probably in the range 2 to 3.5 (Shipboard Scientific Party, 2002) is taken into account (Fig. 2).

Chlorinity of the pore waters universally decreases below the value in bottom seawater, indicating that the upwelling waters are relatively fresh. If the cores had penetrated all the way through the shallow subsurface mixing zone, in which the upwelling pore waters mix with seawater, they would have produced asymptotic profiles, from which the chlorinity of the deep upwelling water could be estimated. Such profiles were found at ODP Site 780 on Conical Seamount and Site 1200 on South Chamorro Seamount. Nonetheless, it is evident that the chlorinity of the upwelling water is not the same at all the sites, as the lowest chlorinity of 464 mmol/kg measured at the Baseball Mitt on Pacman Seamount is lower than that of the asymptotic concentration of 510 mmol/kg in the ODP Site 1200 drillholes on South Chamorro Seamount (Mottl et al., 2003). Neither value is as low as the asymptotic concentration of 260 ± 25 mmol/kg (lowest measured value 234 mmol/kg) at Site 780 on the summit of Conical Seamount (Mottl, 1992).

Sulfate likewise universally decreases, most steeply in the push cores from Cerulean Springs on Pacman Seamount and in a gravity core (GC52) from the summit of South Chamorro Seamount (Fig. 2). Drilling at ODP Site 1200 on this seamount revealed, however, that the deep upwelling water has the same sulfate concentration as seawater (and a 7% higher sulfate/chlorinity ratio) (Mottl et al., 2003), as do the springs sampled there on *Shinkai* Dive 351 (Fryer and Mottl, 1997; Table 3).

Sulfate decreases nearly to zero within the upper 3 to 14 mbsf at Site 1200 because of microbial sulfate reduction, but increases again at greater depth in the upwelling sulfate-rich deep water. At ODP Site 780 on Conical Seamount sulfate is 46 mmol/kg in the deep upwelling water, much higher than in seawater (Mottl, 1992; Table 3). Although sulfate can be reduced inorganically by reaction with $H_2$ produced during serpentinization, microbial sulfate reduction is more likely for the present cores, as there is no evidence for inorganic sulfate reduction below the microbial zone at Sites 1200 and 780. For sites with high Ca, precipitation of gypsum is also a possibility, as it is at ODP Sites 783 and especially 784 on the inactive Torishima Forearc Seamount, where Ca is high and sulfate is low (Figs. 3 and 4). The $\delta^{34}S$ of pore-water sulfate from Site 784, however, is + 31.2 per mil at 11 mmol/kg sulfate, suggesting isotopic fractionation by microbial reduction of seawater sulfate (Mottl and Alt, 1992). In any case it is clear that shallow microbial activity represents a significant complication for inferring the composition of the deep upwelling water, and that results from short cores that do not penetrate beneath the sulfate reduction zone can be misleading for sulfate and related species.

In contrast to chlorinity and sulfate, dissolved Ca increases with depth at some sites (Pacman Baseball Mitt and Blue Moon Seamount) but decreases at others (Pacman subsummit, Big Blue, and South Chamorro, as well as Conical, Seamounts) (Figs. 2 and 3). Correlations with chlorinity (Fig. 3) are generally linear, as would result from convective and diffusive mixing between the upwelling water and ocean bottom water within the shallow subsurface. Reaction could also produce linear relationships over the shallow depth intervals penetrated by these cores, however. The various sites yielded different lines, indicating either that the upwelling end-member solutions differ in composition or that the upwelling speeds differ relative to reaction rates, or both. Based on the presence of both large increases and large decreases in Ca and Sr, we conclude that the composition of the upwelling water differs among the various sites.

We would clearly like to know the composition of the deep upwelling water at each site. These asymptotic compositions are well known for Conical and South Chamorro Seamounts from the deep drill cores (Mottl et al., 2003; Table 3). For the short cores, which did not achieve an asymptotic composition, the usual way to estimate the upwelling end member would be to plot all chemical species against an element that has a known concentration in the end member. The chosen element must be nonreactive within the shallow subsurface mixing zone and its concentration must be different from that in seawater. The usual candidate is Mg because it has a high concentration in the seawater end member and is known to be removed almost completely from solution in many settings within the seafloor. Mg is not so rapidly reactive that its concentration is noticeably changed within the shallow subsurface mixing zone, provided that the waters are upwelling fast enough, usually at a few millimeters per year or faster (e.g., Wheat and Mottl, 2000). Where upwelling is rapid relative to reaction, mixing lines for the various dissolved species can be extrapolated from seawater to a Mg concentration of zero to estimate their concentrations in the upwelling end-member pore water.

For a serpentinite matrix, however, pH is characteristically high (Fig. 5) and Mg is therefore highly reactive. It is rapidly removed into solids at all of our sites, even within the shallow subsurface that was sampled by our cores. (Compare results in Fig. 3 from push cores at Cerulean Springs ["CS"] vs. gravity cores ("BBM"), all from within the Baseball Mitt region on Pacman Seamount.) Except for pH 11.42 measured on push

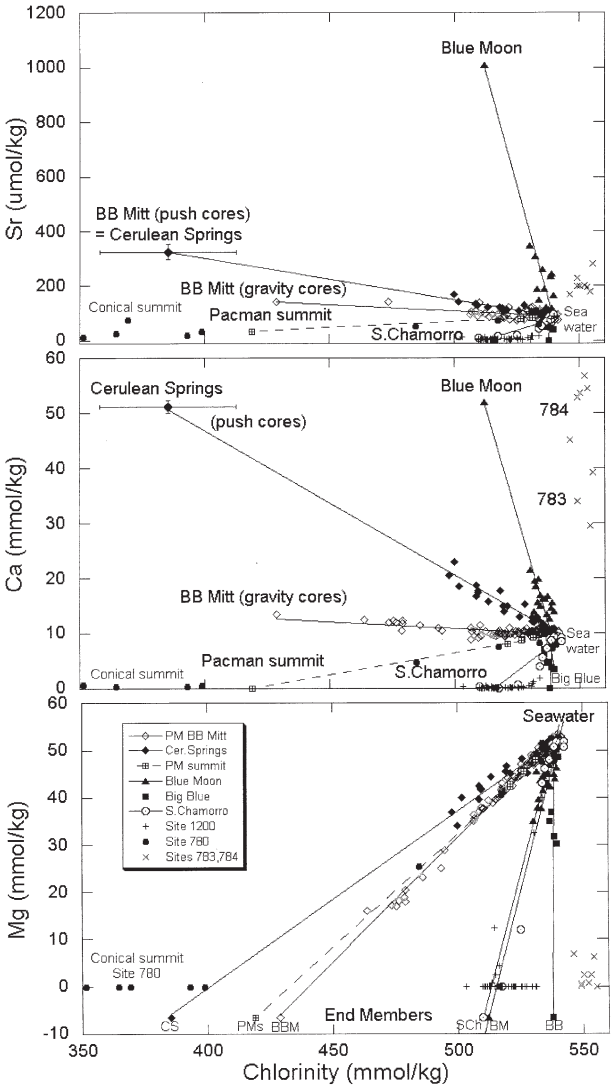


Fig. 3. Chlorinity vs. Mg, Ca, and Sr in pore waters from five active serpentinite mud volcanoes in the Mariana forearc. End-member concentrations are shown as extrapolated values of regression lines to Mg = −6.5 mmol/kg (with some minor correction; see text) for, from left to right, Cerulean Springs (CS) in the Baseball Mitt region on the flank of Pacman Seamount (based on *Jason* push cores), Pacman subsummit (PMs), Pacman Baseball Mitt (BBM, based on gravity and piston cores), and the summits of Blue Moon (BM), and Big Blue (BB) Seamounts. Error bars for Cerulean Springs are 1$\sigma$ about the mean of the three best push cores. Data for South Chamorro (SCh) Seamount include gravity cores, push cores collected from *Shinkai-6500,* and drill cores from ODP Site 1200; the end member is based on the drill-core data. Data for the fifth seamount, Conical, are from ODP Site 780 and are not all shown, as chlorinity as low as 234 mmol/kg was measured there. Also shown are data for ODP Sites 783 and 784 on Torishima Forearc Seamount, an inactive mud volcano in the Izu-Bonin forearc. Plots of chlorinity vs. both Li and F (not shown) closely resemble that for Mg.

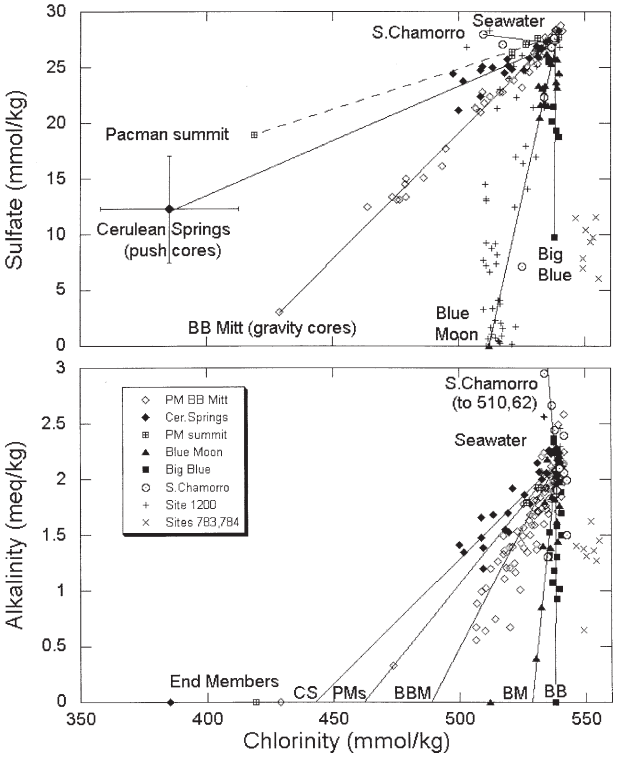


Fig. 4. Chlorinity vs. alkalinity and sulfate in pore waters from four active serpentinite mud volcanoes in the Mariana forearc. See Figure 3 for notes and abbreviations. Like Conical Seamount (not shown), South Chamorro has higher sulfate and much higher alkalinity than seawater. Also shown are data for ODP Sites 783 and 784 on Torishima Forearc Seamount, an inactive mud volcano in the Izu-Bonin forearc.

cores taken by *Shinkai* at the South Chamorro springs (Table 3), the highest pH measured for our short cores was only 9.86. We take the much higher pH of 12.5 measured on deep

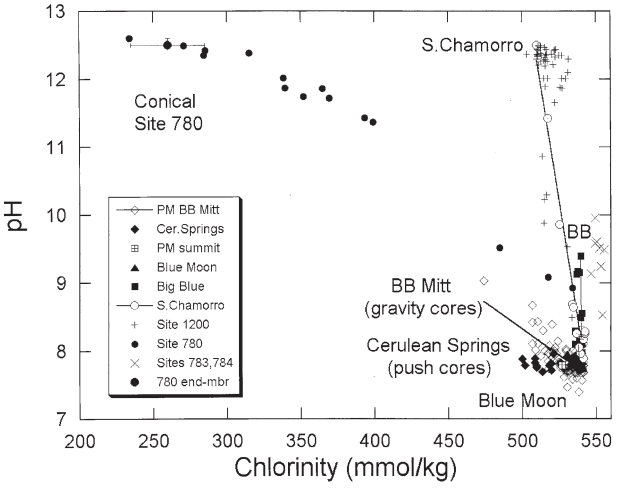


Fig. 5. Chlorinity vs. pH in pore waters from four active serpentinite mud volcanoes in the Mariana forearc. See Figure 3 for notes and abbreviations. Also shown are data for ODP Sites 783 and 784 on Torishima Forearc Seamount, an inactive mud volcano in the Izu-Bonin forearc.

drill cores from ODP Sites 780 and 1200 as more typical for the upwelling, Mg-depleted water. One of the solids that would certainly precipitate on mixing of this water with Mg-rich seawater is brucite, $Mg(OH)_2$. Direct evidence for this process is provided by the brucite chimneys observed at Cerulean Springs in the Baseball Mitt on Pacman Seamount. The assumption that Mg is conservative within the shallow subsurface mixing zone, therefore, necessary for estimating the end-member composition, is clearly violated. Chlorinity is probably conservative, but we do not know its concentration in the upwelling solution.

The best we can do, therefore, is to use Mg and to extrapolate to a concentration less than zero to account for the known removal of this element into brucite in the mixing zone. Thermodynamic calculations using the computer program PHREEQC (Parkhurst and Appelo, 1999) indicate that the total concentration of dissolved hydroxyl and hydroxyl-bearing complexes in the pore waters from ODP Site 1200 on South Chamorro Seamount and Site 780 on Conical Seamount, which have pH of 12.5 ± 0.1 (Mottl et al., 2003), is ~13 ± 5 mEq/kg at the in situ temperature of 2.4°C (at which log $k_w$ is −14.84). Precipitation of this amount of hydroxyl as brucite within the mixing zone sampled by the short cores would remove 6.5 mmol/kg of Mg. We therefore have estimated the composition of the upwelling water at each site (Table 3) by extrapolating mixing (least-squares regression) lines for all chemical species to a Mg concentration of −6.5 mmol/kg, and then making minor adjustments for alkalinity (Fig. 4) and, at two of the four sites, Ca, because they have extrapolated concentrations of slightly less than zero (average −3 mmol/kg). Because brucite precipitation is almost certainly not the only reaction that removes Mg within the mixing zone, these extrapolations are likely minimal. We therefore consider the resulting estimates of composition in Table 3 to be conservative; i.e., the real values probably differ more from seawater than we have estimated in Table 3. In Section 5.1 we check this assumption by comparing results from gravity vs. push cores at the Baseball Mitt site, and from the shallow vs. deep coring (by drilling) at South Chamorro Seamount.

Estimated chlorinity of the upwelling water at the six sites (five plus the Cerulean Springs push cores, collected in the Baseball Mitt but plotted separately from the Baseball Mitt gravity cores) ranges from 386 mmol/kg at Cerulean Springs in the Baseball Mitt on Pacman Seamount to 538 mmol/kg on Big Blue Seamount (Fig. 3). Estimates for Ca range from zero on Big Blue and Pacman summits, similar to the low concentrations known from drilling on Conical and South Chamorro Seamounts (Table 3), to 52 mmol/kg on Blue Moon and at the Baseball Mitt on Pacman Seamount. Sr shows similarly large ranges and correlates with Ca. Blue Moon and South Chamorro Seamounts have wildly divergent Ca and Sr concentrations even though they have nearly identical chlorinity. Plots of Li and F vs. chlorinity (not shown) closely resemble that for Mg, indicating that all three elements are present at very low concentration in the upwelling solution, or that they are highly reactive in the mixing zone, or both.

The alkali elements and B are plotted against chlorinity in Figures 6 to 8. Na varies widely, from higher than in seawater for South Chamorro and Big Blue Seamounts to lower than in seawater for the Baseball Mitt and for Conical and Blue Moon

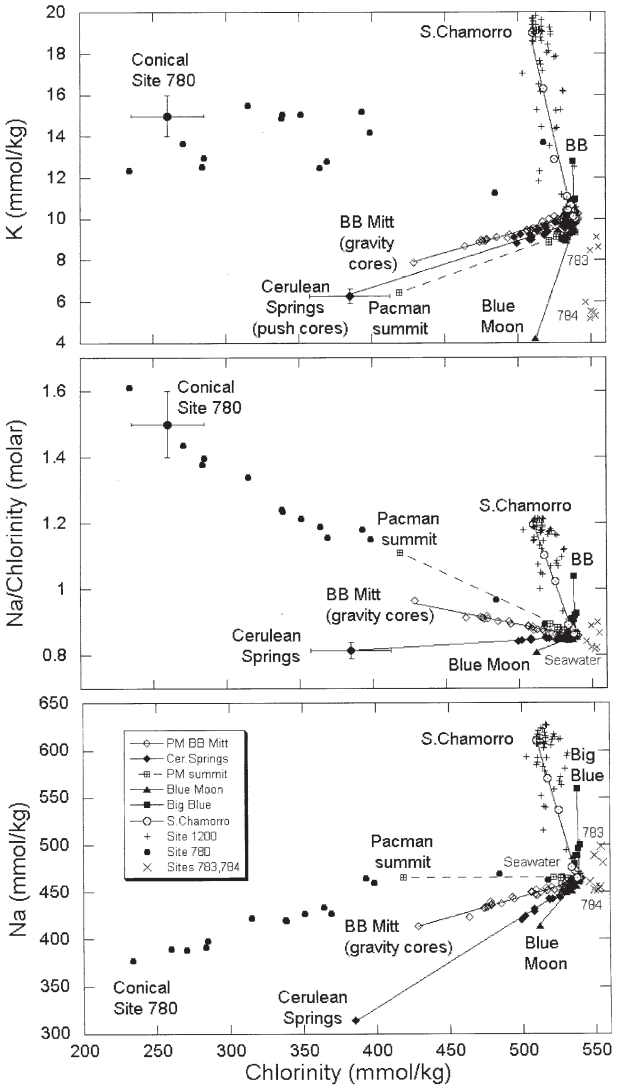


Fig. 6. Chlorinity vs. Na, Na/Chlorinity, and K in pore waters from five active serpentinite mud volcanoes in the Mariana forearc. Also shown are data for ODP Sites 783 and 784 on Torishima Forearc Seamount, an inactive mud volcano in the Izu-Bonin forearc. See Figure 3 for notes and abbreviations. Error bars for the Conical Seamount end member are estimated uncertainties from Mottl et al. (2003).

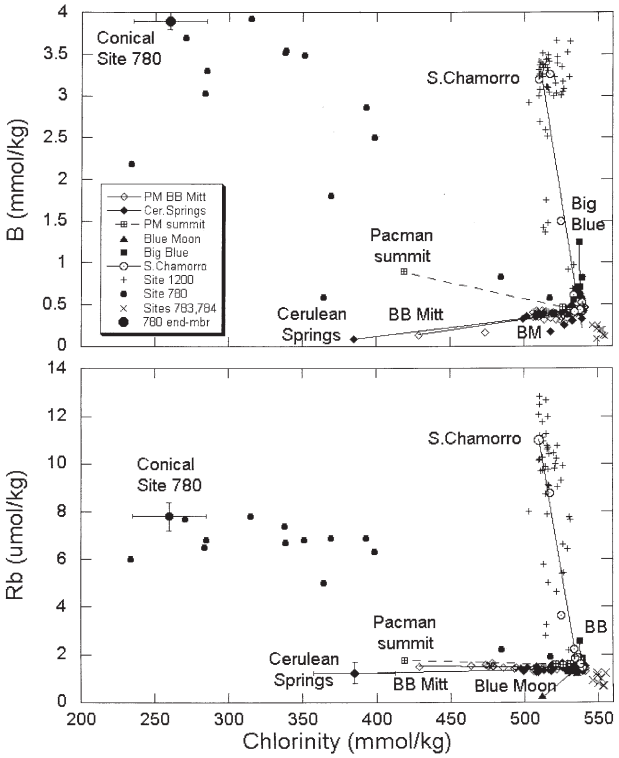


Fig. 7. Chlorinity vs. Rb and B in pore waters from five active serpentinite mud volcanoes in the Mariana forearc. Also shown are data for ODP Sites 783 and 784 on Torishima Forearc Seamount, an inactive mud volcano in the Izu-Bonin forearc. See Figure 3 for notes and abbreviations. Error bars for the Conical Seamount end member are estimated uncertainties from Mottl et al. (2003).

Seamounts. Na at Pacman summit is unchanged. Because of the large changes in chlorinity, however, the Na/chlorinity plots show some different trends: Pacman summit, Conical Seamount, and the gravity cores from the Baseball Mitt join South Chamorro and Big Blue Seamounts in having higher ratios than in seawater. Only Cerulean Springs in the Baseball Mitt and Blue Moon Seamount have lower ratios. Exactly the same pattern is shown for Rb, and nearly so for B, except that B is also lower in the Baseball Mitt gravity cores. K is similar except that it is lower than in seawater at Pacman summit as well. Cs, by contrast, is higher than in seawater at all the sites and shows the largest increase relative to its concentration in seawater. These relationships are shown in Table 3, where concentrations higher than in seawater for these species are shown in bold type.

While these extrapolations are large, there can be no doubt that the first-order differences in composition of the upwelling pore waters among the sites are real. The correlations with Mg are good, with average $r^2$ for the six sites of 0.90 or better for chlorinity (0.93), sulfate (0.90), alkalinity (0.95), Na (0.92), Na/chlorinity (0.95), Li (0.92), K (0.91), Cs (0.93), Ca (0.98), Sr (0.90), B (0.95), Si (0.92), and F (0.95). Correlations are not as good for $^{87}Sr/^{86}Sr$ (0.81), Rb (0.80), Ba (0.68), $\delta^{18}O$ (0.52), Fe (0.36), and Mn (0.31).

### 4.2. Effect of Reaction within the Shallow Subsurface Mixing Zone

The effect of reaction in the shallow subsurface can be evaluated by comparing the two sets of cores from the Baseball Mitt: the push cores collected by the ROV *Jason* at Cerulean Springs, with their much higher chemical gradients (Fig. 2), used to estimate the end-member composition in Table 3, vs. the gravity and piston cores (Fryer et al., 1999). Because these cores were all collected in the same locality we can assume that both sets reflect the same upwelling water, and that the differences result from reaction within the shallow subsurface where the upwelling solutions mix with the overlying seawater. Because upwelling is much faster at Cerulean Springs, any reaction within the mixing zone would have much less effect on the composition of the water sampled there.

End-member concentrations of chlorinity, Ca, and Sr, when

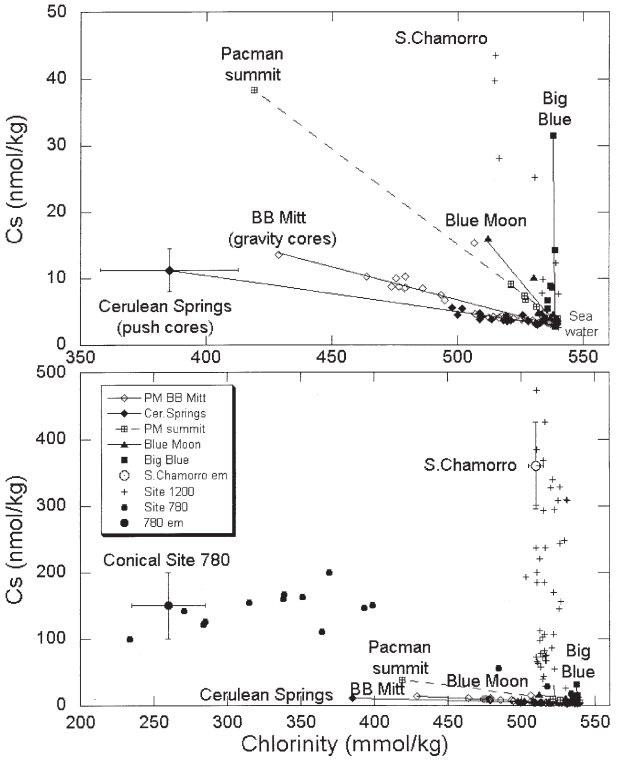


Fig. 8. Chlorinity vs. Cs in pore waters from five active serpentinite mud volcanoes in the Mariana forearc. See Figure 3 for notes and abbreviations. Part of the lower figure is expanded in the upper figure, on both axes.

estimated by extrapolation against Mg, appear to be different for the two sets of Baseball Mitt cores (Fig. 3). (Note that extrapolating Ca and Sr to the end-member chlorinity for Mg = −6.5 mmol/kg is mathematically equivalent to extrapolating against Mg. We show plots against chlorinity because it is conservative and Mg is not. We thus restrict the effects of reaction to a single variable in any given plot.) As chlorinity is probably conservative in these cores, the difference almost certainly results from greater loss of Mg, Ca, and Sr from the more slowly upwelling waters sampled by the gravity cores, as concluded by Fryer et al. (1999). The minimum losses can be estimated from the difference. Ba, Si, and F show a similar pattern (not shown; compare values in Table 3 with those in the first column in Tables 4 and 5) indicating that they also are removed in the mixing zone.

Like Mg, Ca, and Sr, alkalinity and sulfate also show consistently lower concentrations for a given chlorinity in the gravity and piston cores from the Baseball Mitt than in the *Jason* push cores at Cerulean Springs (Fig. 4), implying that they too are lost by reaction within the mixing zone. Both species appear to decrease relative to seawater at all sites except South Chamorro Seamount (Fig. 4) and Conical Seamount (not shown; see Table 3), which show moderate to large increases in alkalinity and sulfate (sulfate/chlorinity at South Chamorro). We have already noted, however, that in short cores the trends for sulfate can be misleading, as shown by the low sulfate in most of the samples from ODP Site 1200 compared with the deeper asymptotic concentration that is slightly higher than in seawater (Fig. 4 and Table 3). Except for South Chamorro and Big Blue Seamounts, all of the extrapolated end-member alkalinity concentrations are significantly negative, reinforcing the conclusion that alkalinity is lost by reaction within the mixing zone. This loss is doubtless due to precipitation of $CaCO_3$, mainly in the form of aragonite needles that are abundant within this zone in all the cores. (See also Mottl, 1992; Shipboard Scientific Party, 2002; Mottl et al., 2003.) One minor correction we have made to the end-member compositions in Table 3 restores the negative alkalinities to zero and adds similar equivalents of Ca, ranging from 1.5 mEq/kg for Cerulean Springs and Pacman Seamount summit to 4.4 mEq/kg for Blue Moon Seamount. A second minor correction necessary for only two sites restores negative Ca values to zero by adding equivalent sulfate, 1.6 mmol/kg for Pacman summit and 7.6 mmol/kg for Big Blue Seamount. We restored Ca along with sulfate under the assumption that the negative Ca concentrations were caused either by gypsum precipitation or by microbial sulfate reduction. (The latter reaction generates carbonate alkalinity, as shown in the footnote to Tables 4 and 5, which would precipitate additional Ca as $CaCO_3$.) We have searched for gypsum in the cores by X-ray diffraction but have so far not found it.

Comparison of the Jason push cores from Cerulean Springs with the other cores from the Baseball Mitt on Pacman Seamount indicates that Na and Na/chlorinity are significantly lower in the more rapidly upwelling pore waters at Cerulean Springs (Fig. 6). So are K and Cs, but just barely; Rb and B (and Li, not shown) are indistinguishable in the two data sets within uncertainty (Figs. 7, 8). In contrast to Mg, Ca, Sr, Ba, Si, F, alkalinity, and sulfate, therefore, which are taken up into the solids, Na and to a minor extent K and Cs are apparently leached from solids within the mixing zone sampled by these short cores. Li, Rb, and B are conservative (and K and Cs are nearly so).

### 4.3. Isotopes of Oxygen and Strontium

Oxygen and Sr isotopic data sets are not as complete as for the other chemical species, but the results are fairly consistent (Fig. 9). $\delta^{18}O$ is more positive than in seawater at South Chamorro and Conical Seamounts and in the Baseball Mitt on the flank of Pacman Seamount, with values ranging from + 0.5 per mil at the Baseball Mitt to + 4.5 per mil at Conical Seamount. Values measured at Pacman summit and at Blue Moon and Big Blue Seamounts are indistinguishable from ambient ocean bottom water. Only at ODP Site 784 on the inactive Torishima Forearc Seamount are values clearly lower than in seawater; these waters result from reaction of seawater with harzburgite at 4° to 11°C (Mottl, 1992; Mottl et al., 2003). Such reaction may explain why the seawater end member, as inferred from the pore water samples collected nearest to the seafloor, has a slightly negative $\delta^{18}O$ of about −0.4 per mil.

Measured Sr isotopic ratios are all lower than in seawater, ranging as low as 0.70523 for pore water from South Chamorro Seamount (Fig. 9). Extrapolated values are as low as 0.70265, but these are not very reliable.

Table 4. Composition of ascending pore water at Baseball Mitt on Pacman Seamount: shallow subsurface reactions inferred by comparing gravity cores (slow upwelling) vs. *Jason* push cores from Cerulean Springs (faster upwelling).

| | | Correct for: | | | | | | | | | |
|---|---|---|---|---|---|---|---|---|---|---|---|
| | Pacman[a] BB Mitt gravity cores | 1 Chlorinity | 2 $CaCO_3$ ppt′n | 3[b] $SO_4$, Ca removal | 4 Ca-Na exchange | 5 $Mg(OH)_2$ ppt′n | 6 Mg-K exchange | 7 Mg-Na exchange | Pacman[a] BB Mitt push cores | $\pm 1\sigma$ for best 3 cores | Effects of shallow reactions |
| 41 to 100 samples from as deep as 2.76 mbsf | | | | | | | | | 15 samples from as deep as 0.22 mbsf | | |
| pH | 9.38 | 9.54 | 9.54 | 9.54 | 9.54 | 12.5 | 12.5 | 12.5 | 12.5[c] | | down |
| | mEq/kg: | | | | | | | | | | |
| Alkalinity | −2.1 | −3.8 | 0.02 | 0.02 | 0.02 | 13 | 13 | 13 | 13 | | loss |
| Carb.sp. | −2.1 | −3.8 | 0 | 0 | 0 | 0 | 0 | 0 | 0 | | loss |
| OH-sp. | 0.01 | 0.02 | 0.02 | 0.02 | 0.02 | 13 | 13 | 13 | 13 | | loss |
| | mmol/kg: | | | | | | | | | | |
| Chlorinity | 429 | 386 | 386 | 386 | 386 | 386 | 386 | 386 | 386 | 27 | unchanged |
| Sulfate | 3.1 | −6.8 | −6.8 | 12.3 | 12.3 | 12.3 | 12.3 | 12.3 | 12.3 | 4.8 | loss |
| Mg | −6.5 | −29.7 | −29.7 | −29.7 | −29.7 | −23.3 | −22.9 | 0 | 0 | 0.01 | loss |
| Ca | 12.4 | 13.5 | 15.3 | 34.4 | 51.2 | 51.2 | 51.2 | 51.2 | 51.2 | 1.1 | loss |
| Na | 414 | 395 | 395 | 395 | 362 | 362 | 362 | 316 | 314 | 23 | gain |
| Na/Cl | 0.97 | 1.03 | 1.03 | 1.03 | 0.94 | 0.94 | 0.94 | 0.82 | 0.82 | 0.02 | gain |
| K | 7.9 | 7.0 | 7.0 | 7.0 | 7.0 | 7.0 | 6.3 | 6.3 | 6.3 | 0.3 | slight gain |
| | $\mu$mol/kg: | | | | | | | | | | |
| | | Summary of changes resulting from shallow reactions, in mEq/kg, from Column 7 (unreacted) to Column 1 (reacted) above (see Section 5.1.1): | | | | | | | Total for row | | Net Effect |
| Li | 10.5 | | | | | | | | | | |
| Rb | 1.5 | | | | | | | | | | |
| Cs | 0.014 | Alkalinity | −4 | | | −13 | | | −17 | | loss |
| Sr | 141 | Sulfate | | −38 | | | | | −38 | | loss |
| Ba | 0.24 | Ca | −4 | −38 | −34 | | | | −75 | | loss |
| B | 133 | Mg | | | | −13 | −0.7 | −46 | −59 | | loss |
| Si | 0 | K | | | | | 0.7 | | 1 | | slight gain |
| F | 0 | Na | | | 34 | | | 46 | 79 | | gain |
| Mn | 0.09 | Charge balance | | | | | | | 0 | | |
| Fe | 0 | | | Minor and trace elements: Cs rises slightly. | | | | | | | |
| $\delta^{18}O$ | +0.52 o/oo SMOW | | | (See Table 3 for results from push cores.) Sr, Ba, Si, and F drop. | | | | | | | |
| $^{87}Sr/^{86}Sr$ | 0.70435 | | | | | Li, Rb, B, Mn, Fe, and $^{87}Sr/^{86}Sr$ are unchanged within $1\sigma$. | | | | | |

[a] Composition was determined by extrapolating to Mg = −6.5 mmol/kg, to account for precipitation of brucite on mixing with seawater.
[b] "$SO_4$, Ca removal" represents the net effect of either gypsum precipitation or alkalinity production by sulfate reduction followed by $CaCO_3$ precipitation: $SO_4^{2-} + CH_4 + OH^- \rightarrow CO_3^{2-} + HS^- + 2H_2O$ and $Ca^{2+} + CO_3^{2-} \rightarrow CaCO_3$
[c] pH is assumed to be 12.5, equivalent to 13 mEq/kg total hydroxyl species at 2.4°C, from thermodynamic calculations using PHREEQC.

## 5. DISCUSSION

### 5.1. Quantifying Reaction in the Shallow Subsurface Mixing Zone

Three sets of data allow us to quantify reactions in the mixing zone using simple mass balance and stoichiometry.

#### *5.1.1. Baseball Mitt Site on Pacman Seamount*

The differences between the rapidly upwelling pore water at Cerulean Springs, sampled by the *Jason* push cores and used to estimate the Baseball Mitt end member in Table 3, and the more slowly upwelling water from the Baseball Mitt sampled by the gravity and piston cores, are illustrated in Figures 2 to 8 and summarized above. In Table 4 we quantify these differences for the major species and attempt to infer the reactions that account for them, which occur as upwelling pore water of a uniform composition within the Baseball Mitt mixes convectively and diffusively with the overlying seawater in the shallow subsurface.

The end-member compositions of the upwelling water in Table 3 were determined by extrapolating to a Mg concentration of −6.5 mmol/kg to account for precipitation of brucite in the mixing zone. Any negative concentrations of alkalinity and Ca were then adjusted upward to zero by minor addition of Ca and sulfate, respectively, as discussed above. In Table 4 the two end-member compositions so determined from the Baseball Mitt site bracket the seven-step procedure we used, from the slowly upwelling (more reacted) gravity-core end member on the left to the rapidly upwelling (less reacted) push-core end member (also given in Table 3) on the right. The first step is to reconcile chlorinity, as the extrapolated value for the gravity cores of 429 mmol/kg is much higher than the value of 386 mmol/kg for the push cores (Fig. 3) because of greater loss of Mg from the more slowly upwelling solutions. Further extrapolation of the gravity-core data to the push-core chlorinity of 386 mmol/kg yields a Mg concentration of −29.7 mmol/kg, much lower than the value of −6.5 assumed initially and reinforcing the conclusion that this assumption was a conser-

Table 5. Composition of ascending pore water at South Chamorro Seamount summit: shallow subsurface reactions inferred by comparing Gravity Core 52 with ODP Site 1200 (asymptotic) composition.

| | South Chamorro GC52[a] gravity core | Correct for: 1 Chlorinity | 2[b] Alk'y prod'n | 3[b] $SO_4$, Ca removal | 4 $Mg(OH)_2$ ppt'n | 5 Ca-Na exchange | 6 K-Ca exchange | 7 Mg-Ca exchange | South Chamorro Site 1200[a] deep water | Est'd ± | Effects of shallow reactions |
|---|---|---|---|---|---|---|---|---|---|---|---|
| 4 to 11 samples from as deep as 0.37 mbsf | | | | | | | | | 53 samples from as deep as 71 mbsf | | |
| pH | 10.05 | 10.25 | 10.25 | 10.25 | 12.5 | 12.5 | 12.5 | 12.5 | 12.5[c] | | down |
| | mEq/kg: | | | | | | | | | | |
| Alkalinity | 50.8 | 77.2 | 49.3 | 49.3 | 62 | 62 | 62 | 62 | 62 | 8 | slight gain* |
| Carb. sp. | 48.7 | 73.9 | 46 | 46 | 46 | 46 | 46 | 46 | 46 | 7 | gain |
| OH-sp. | 0.05 | 0.08 | 0.08 | 0.08 | 13 | 13 | 13 | 13 | 13 | | loss |
| | mmol/kg: | | | | | | | | | | |
| Chlorinity | 519 | 510 | 510 | 510 | 510 | 510 | 510 | 510 | 510 | 5 | unchanged |
| Sulfate | −2.7 | −18.5 | −4.5 | 28.0 | 28.0 | 28.0 | 28.0 | 28.0 | 28 | 1 | loss |
| Mg | −6.5 | −36.4 | −36.4 | −36.4 | −29.9 | −29.9 | −29.9 | −0.2 | <0.01 | 0.01 | loss |
| Ca | −3.2 | −8.7 | −8.7 | 23.7 | 23.7 | 31.1 | 29.7 | 0 | 0.3 | 0.1 | loss |
| Na | 570 | 625 | 625 | 625 | 625 | 610 | 610 | 610 | 610 | 10 | slight gain* |
| Na/Cl | 1.10 | 1.22 | 1.22 | 1.22 | 1.22 | 1.20 | 1.20 | 1.20 | 1.20 | 0.02 | slight gain* |
| K | 14.2 | 16.2 | 16.2 | 16.2 | 16.2 | 16.2 | 19.0 | 19.0 | 19 | 1 | slight loss |
| | μmol/kg: | | | | | | | | | | |
| Li | 4.5 | Summary of changes resulting from shallow reactions, in mEq/kg, from column 7 (unreacted) to Column 1 (reacted) above (see Section 5.1.2): | | | | | | | Total for row | | Net Effect |
| Rb | 4.6 | | | | | | | | | | |
| Cs | 0.014 | Alkalinity | 28 | | −13 | | | | 15 | | slight gain* |
| Sr | 0 | Sulfate | −28 | −65 | | | | | −93 | | loss |
| Ba | 0.05 | Ca | | −65 | | −15 | 3 | 59 | −17 | | loss |
| B | 1990 | Mg | | | −13 | | | −59 | −72 | | loss |
| Si | 0 | K | | | | | −3 | | −3 | | slight loss |
| F | 18.4 | Na | | | | 15 | | | 15 | | slight gain* |
| Mn | 0.09 | Charge balance | | | | | | | 0 | | |
| Fe | 1.0 | Minor and trace elements: Li, Rb, B, Sr, Ba, Si, F, and Fe drop. | | | | | | | | | |
| $\delta^{18}O$ | +0.7 o/oo SMOW | (See Table 3 for results from Site 1200.) Mn is unchanged within 1σ | | | | | | | | | *probably insignificant |
| $^{87}Sr/^{86}Sr$ | 0.7092 | | | | | | | | | | |

[a] Composition of GC52 was determined by extrapolating to Mg = −6.5 mmol/kg, to account for precipitation of brucite on mixing with seawater. Site 1200 data are from Shipboard Scientific Party (2002) and Mottl et al. (2003).

[b] "$SO_4$, Ca removal" represents the net effect of alkalinity production by sulfate reduction followed by $CaCO_3$ precipitation: $SO_4^{2-} + CH_4 + OH^- \rightarrow CO_3^{2-} + HS^- + 2H_2O$ and $Ca^{2+} + CO_3^{2-} \rightarrow CaCO_3$

[c] pH 12.5 is equivalent to 13 mEq/kg total hydroxyl species at 2.4°C, from thermodynamic calculations using PHREEQC.

vative one, as we intended it to be. Note that the inferred loss of −29.7 mmol/kg Mg from the more slowly upwelling waters sampled by the piston and gravity cores does not require that this much Mg also has been lost from the push cores at Cerulean Springs, as these waters are upwelling much more rapidly and have clearly reacted less on mixing. In column 1 of Table 4 all concentrations have been adjusted by extrapolation to Mg = −29.7. These concentrations are based on linear correlations displayed by data from the short cores, whereas the actual correlations are surely nonlinear, as would be seen if the cores had penetrated more deeply. For this reason the absolute values derived are not meaningful, but the changes of one species relative to another should be.

In column 2 we correct for $CaCO_3$ precipitation in the mixing zone by adjusting the negative carbonate alkalinity upward to zero along with an equivalent amount of Ca, as discussed above. In column 3 we correct either for gypsum precipitation or for possible microbially mediated sulfate reduction and attendant production of carbonate alkalinity and $CaCO_3$ precipitation, by adjusting sulfate upward to the concentration in the push-core end member, along with equivalent Ca. Although we have not found gypsum in these cores, thermodynamic calculations using PHREEQC (Parkhurst and Appelo, 1999) indicate that the end-member solution at Cerulean Springs containing 51.2 mmol/kg Ca would become saturated with gypsum at a sulfate concentration of only 16 mmol/kg at 2.4°C, remarkably close to the 12 mmol/kg estimated in Tables 3 and 4. In column 4 we adjust Ca upward further to the final push-core value in exchange for Na, as Na is the only cation sufficiently abundant to allow for the large additional increase in Ca necessary to match the push-core data, and Na must decrease in any case. This exchange of Ca for Na in the mixing zone probably involves leaching of Na from clay minerals in the thin volcanic ash-rich layer of sediment that overlies serpentinite in most of the cores, as noted above. In column 5 we correct for brucite precipitation by adjusting total alkalinity upward to 13 mEq/kg, appropriate for pH 12.5 as discussed above, along with equivalent Mg. We assume that pH of the upwelling pore water is 12.5 because this is the asymptotic value measured in the deep drill cores from Conical and

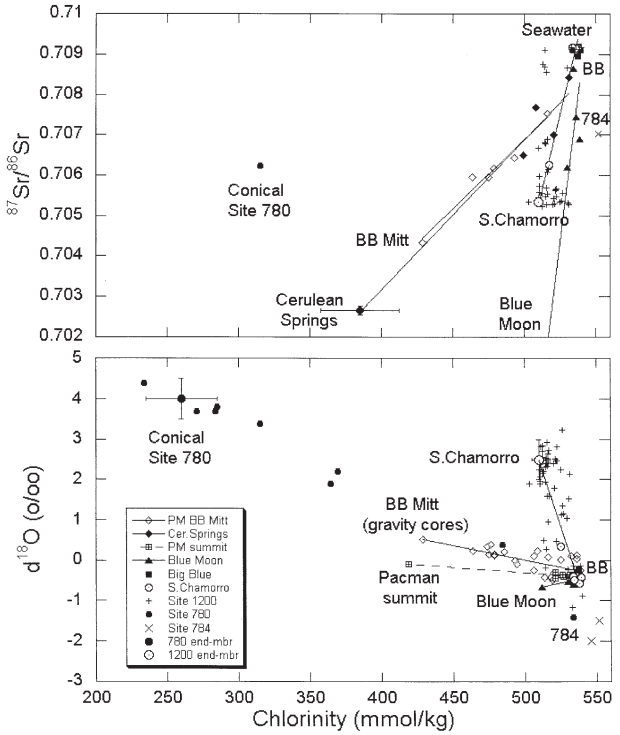


Fig. 9. Chlorinity vs. $\delta^{18}O$ and $^{87}Sr/^{86}Sr$ in pore waters from five active serpentinite mud volcanoes in the Mariana forearc. Also shown are data for ODP Site 784 on Torishima Forearc Seamount, an inactive mud volcano in the Izu-Bonin forearc. See Figure 3 for notes and abbreviations. Error bars for the Conical and South Chamorro Seamount end members are estimated uncertainties from Mottl et al. (2003). Data are from J. Martin (this study), Haggerty and Chaudhuri (1992, Sr at Sites 780 and 784), Benton (1997, O at Sites 780 and 784), Bickford and Siegel (personal communication; Sr at Site 1200) and Mottl et al. (2003, O at Site 1200).

South Chamorro Seamounts. In column 6 we make a trivial, pro forma downward adjustment of K to the concentration in the push cores, in exchange for Mg, as Mg still needs to rise. In column 7 we adjust Mg upward to zero in exchange for additional Na, presumably leached from clays. This final correction brings Na nearly to its concentration in the push-core end member, as would have to be the case because of the constraint of charge balance.

This set of reactions reconciles the slowly upwelling pore water with the more rapidly upwelling water at Cerulean Springs, all within the Baseball Mitt, and it or something like it must be happening within the shallow subsurface mixing zone there. The net results are summarized in the lower half of Table 4 and comprise large losses from solution, in order of extent, of 1) Ca, as $CaCO_3$ and gypsum and in exchange for Na; 2) Mg, in exchange for Na and as brucite; 3) sulfate, removed either as gypsum or as reduced sulfur; and 4) alkalinity, as brucite and $CaCO_3$. These losses are balanced by substantial leaching of Na, presumably from clay minerals in the sediment layer that overlies serpentinite in most of the cores. Also lost are Sr, Ba, Si, and F. K and Cs appear to rise slightly but the increases may be insignificant. Li, Rb, and B are indistinguishable between the two sets of cores within the uncertainty of the extrapolation. So are Mn, Fe, and $^{87}Sr/^{86}Sr$, largely because of poor correlation with Mg for these latter species.

### 5.1.2. *Summit of South Chamorro Seamount*

A similar exercise can be performed for the summit of South Chamorro Seamount by comparing the asymptotic composition of the ascending pore water, as sampled at considerable depth by drilling at ODP Site 1200, with an extrapolated end-member solution from our gravity coring (Table 5). The results can be expected to differ from those in Table 4 because the upwelling pore water at South Chamorro Seamount has high alkalinity, twenty times that in seawater, and little Ca, whereas the water at the Baseball Mitt site on Pacman Seamount has essentially no carbonate alkalinity and five times more Ca than in seawater.

As in Table 4, the seven steps are bracketed on the left by the (more reacted) end-member pore water for a gravity core, determined as in all the other cases by extrapolating measured concentrations to Mg = −6.5 mmol/kg, and on the right by the (unreacted, i.e., no shallow reaction) end-member composition for Site 1200. The data from Site 1200 are the most definitive obtained to date from the Mariana forearc serpentinite seamounts because three holes were drilled with increasing distance from a spring and two of these penetrated all the way through a near-surface zone of microbial sulfate reduction to yield asymptotic concentrations for most chemical species (Mottl et al., 2003). We again start by correcting chlorinity in column 1, to the asympototic concentration of 510 ± 5 mmol/kg. This concentration is achieved at a Mg concentration of −36.4 mmol/kg, not far from the −29.7 mmol/kg needed for the Baseball Mitt site (Table 4), again indicating that our initial extrapolation to Mg = −6.5 was a conservative underestimate of Mg loss on mixing.

The correction for chlorinity in column 1 raises the alkalinity from below that at Site 1200 to above it, requiring a downward adjustment in total and carbonate alkalinity in column 2 to match the final values at Site 1200. This implies that alkalinity is produced in the mixing zone, as would result from the microbial sulfate reduction known to occur there (Mottl et al., 2003). Accordingly we have adjusted sulfate upward in column 2 by an equivalent amount. In column 3 we adjust sulfate upward further to its final value, this time along with equivalent Ca, assuming that this increment of carbonate alkalinity produced was precipitated as $CaCO_3$. In column 4 we correct for brucite precipitation as in Table 4, by adjusting total alkalinity upward to 13 mEq/kg, appropriate for pH 12.5 as observed at Site 1200, along with equivalent Mg. In column 5 we adjust Na downward to its final value in exchange for Ca, the same exchange effected in column 4 of Table 4. In column 6 we make a negligible adjustment of K to its final value, this time upward and in exchange for Ca. In column 7 we make the final upward adjustment for Mg to essentially zero, this time in exchange for Ca, which decreases to its final value near zero, as it must because of the charge balance constraint.

The net results of the adjustments necessary to reconcile the gravity cores with the drill cores are summarized in the lower half of Table 5. They comprise large losses from solution, in order of extent, of 1) sulfate, reduced to bisulfide; 2) Mg, in exchange for Ca and as brucite; and 3) Ca, as $CaCO_3$ and in exchange for Na. These losses are balanced by relatively mod-

est leaching of Na, in exchange for Ca, and production of alkalinity by microbial sulfate reduction. As at the Baseball Mitt site, Sr, Ba, Si, and F are lost from solution, but at South Chamorro they are joined by Li, K, Rb, B, and Fe. Only Mn is indistinguishable in the two types of cores, largely because of its poor correlation with Mg in the sampled pore waters.

#### 5.1.3. *Three Drillholes at ODP Site 1200 on South Chamorro Seamount*

By comparing cores from three holes drilled with increasing distance from a spring at ODP Site 1200 on the summit of South Chamorro Seamount, Mottl et al. (2003) demonstrated that K, Rb, and $^{18}O/^{16}O$ were conservative within the mixing zone; Na and B were leached from the serpentinite mud; and Mg, Ca, Sr, Li, and Si were taken up into the solids. Even at this site of active serpentinite protrusion, reaction with material other than serpentinite probably plays a role, as the upper 3 mbsf in Hole 1200D farthest (80 m) from the spring is rich in hemipelagic sediment. Most of the reaction, however, takes place much deeper than that and must involve the serpentinite mud.

#### 5.1.4. *Summary and Implications of Reaction in the Mixing Zone*

The changes that are consistent among all three examples include large losses from solution of 1) Ca, as $CaCO_3$ and in exchange for Na; 2) Mg, in exchange for Na or Ca and as brucite; 3) sulfate, reduced by microbes or precipitated as gypsum; 4) Sr, Ba, Si, and F. Under similar conditions of flow and mixing, sites with high alkalinity and low Ca (South Chamorro and Conical Seamounts) have the potential to precipitate more than twice as much $CaCO_3$ as those with low alkalinity and high Ca (Pacman Baseball Mitt and Blue Moon Seamount). The latter sites may also precipitate gypsum, which is unlikely ever to reach saturation at the former sites. Na is consistently leached from the solids into solution, even where an upper layer of hemipelagic sediment is absent and serpentinite mud is the only solid, as in the deep drillholes at Site 1200. Whereas the harzburgite protolith contains little or no Na, the serpentinite mud apparently does (Table 2). This Na probably resides in the few percent of mafic clasts such as those found in serpentinite mud at ODP Sites 778 to 780 on Conical Seamount (Johnson, 1992) and at Site 1200 on South Chamorro Seamount (Shipboard Scientific Party, 2002). K and $^{18}O/^{16}O$ are relatively unreactive. Cl, which is probably leached from iowaite in Hole 1200D (Fryer and Mottl, 1992; Mottl et al., 2003), alkalinity, Li, Rb, and B behave inconsistently in the three examples.

A major implication of this exercise is that the initial extrapolations to Mg = −6.5 mmol/kg, used to estimate the upwelling end-member compositions for Pacman Baseball Mitt, Pacman subsummit, and Blue Moon and Big Blue Seamounts in Table 3, are surely minimal. Although we have compared the gravity cores from Baseball Mitt with the push cores from Cerulean Springs to infer reactions in the mixing zone, these same reactions must have affected pore waters from Cerulean Springs as well, although to a lesser extent because the effects would be diluted by the more rapidly upwelling water. The actual composition of upwelling pore water can only be determined by sampling at greater depth than our short cores achieved, or at springs flowing more rapidly than we have sampled to date. Such deep sampling has been achieved at South Chamorro and Conical Seamounts, by drilling. The other end-member compositions in Table 3 almost certainly represent conservative underestimates of the real amount of change relative to seawater.

### 5.2. Chemical Trends in Upwelling Water across the Mariana Forearc

The composition of upwelling pore water at the six sites on five seamounts in Table 3 varies drastically and systematically across the Mariana forearc (Fig. 10). The two sites closest to the trench axis, the Baseball Mitt site on the flank of Pacman Seamount (52 km distant) and the summit of Blue Moon Seamount (55 km), have waters with Ca and Sr much higher than in seawater (values in bold type in Table 3), and carbonate alkalinity, sulfate, Na/Cl, K, Rb, and B lower than in seawater. The two sites farthest from the trench axis, South Chamorro (85 km) and Conical Seamounts (90 km), have waters that show the opposite directions of change: Ca and Sr are much lower than in seawater whereas alkalinity, sulfate (sulfate/Cl for South Chamorro), Na/Cl, K, Rb, and B are higher to much higher than in seawater. The two sites at intermediate distances from the trench axis, Pacman subsummit (64 km) and Big Blue Seamount (70 km), have intermediate compositions: Ca and Sr are much lower than in seawater, but carbonate alkalinity and sulfate also are apparently lower. K is lower at Pacman subsummit but higher at Big Blue Seamount. Na/Cl, Rb, and B are all higher than in seawater at these two intermediate sites, as at the two seamounts farthest from the trench. Chlorinity varies greatly from site to site but this variation is not systematic with distance from the trench. Cs is higher than in seawater at all the sites and increases with distance from the trench.

We interpret these trends as resulting from progressive devolatilization of the subducting slab with increasing depth and temperature beneath the forearc (Fryer et al., 1999). Our estimates of depth to the top of the downgoing plate for distances of 52 to 90 km from the trench axis range from 16 to 29 km (Table 3) based on earthquake depths (Hussong and Fryer, 1981; Seno and Maruyama, 1984); these depths correspond to a slab dip of 17.5° for this shallow part of the subduction zone but are highly uncertain. The systematic variations in spring composition are exactly what would be expected for devolatilization of sediments and altered oceanic crust at the top of the subducting plate with increasing temperature (e.g., Bebout, 1995; Ryan et al., 1996; Bebout et al., 1999). These systematic variations further imply that the solutions ascend more or less vertically from the source region rather than traveling long distances laterally along the décollement before ascending.

Close to the trench pore water in the subducted sediment is squeezed out by compaction. This water should have chlorinity near that of seawater and so is not the ascending water we have sampled in this study. Most sediment compaction should occur shallower and much closer to the trench than the mud volcanoes we have sampled. At 52 to 90 km from the trench all of the upwelling pore waters have lower chlorinity than seawater,

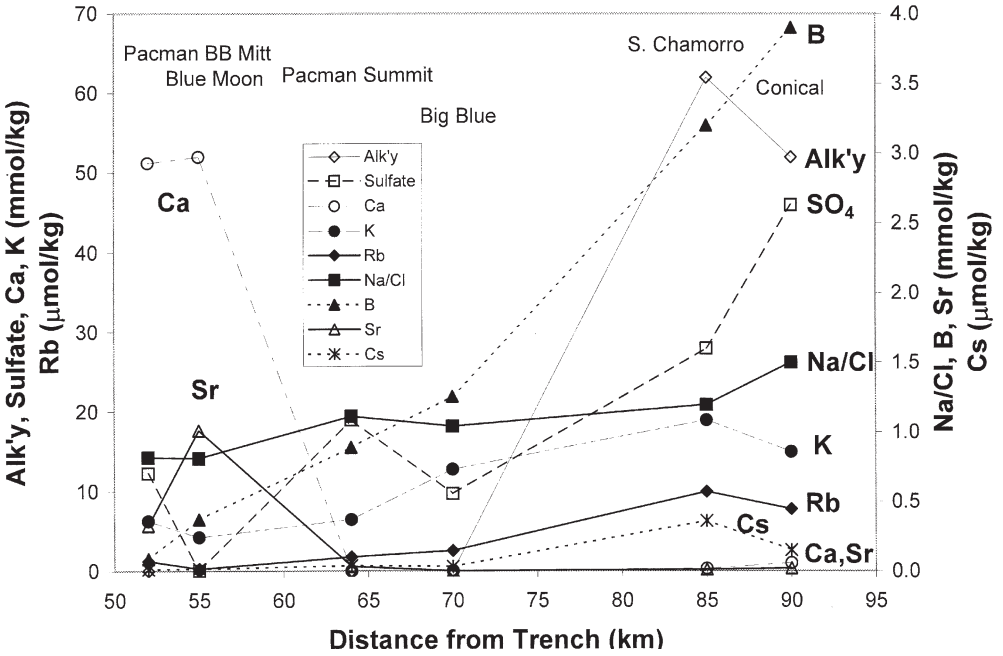


Fig. 10. Concentrations of alkalinity, sulfate, Na/Chlorinity, K, Rb, Cs, B, Ca, and Sr in upwelling pore water sampled from six sites on five serpentinite mud volcanoes in the Mariana forearc, and their variation with distance from the trench across the outer forearc, from Table 3.

indicating that dehydration of the subducting plate has begun at depth. The initial chlorinity of waters of dehydration at depth is not known, but it is probably quite low, such that these solutions may be essentially fresh. As they ascend from the subducting slab through the overlying mantle wedge they become saltier by loss of $H_2O$ to serpentinization, which continues all the way to the seafloor, as indicated by the high pH and the continued presence of unaltered harzburgite there (Shipboard Scientific Party, 1990, 2002). Despite massive loss of $H_2O$ to serpentinization the solutions arrive at the seafloor with chlorinity that is still lower than that of seawater. This chlorinity probably originates as residual pore water that was not squeezed out by sediment compaction and was subsequently leached by waters of dehydration. Some of it may also originate from seawater that could be entrained at relatively shallow depth during ascent. Either process could account for some seawater Sr, with high $^{87}Sr/^{86}Sr$, in the upwelling water. Variable amounts of entrainment vs. serpentinization along the flow path could readily account for the large but unsystematic variability in chlorinity of the upwelling solutions from site to site.

Besides $H_2O$, the chemical species most enriched at the two sites closest to the trench are Ca and Sr. The source of these elements could be oceanic crust (including sediment) at the top of the subducting slab, but the large enrichment of Ca (but not Sr) in pore water from the inactive Torishima Forearc Seamount (Fig. 3) indicates that Ca could just as well be leached from peridotite. Even depleted harzburgite contains some Ca (Table 2), mainly in the 0 to 2% clinopyroxene present in these rocks. In the absence of high carbonate alkalinity these elements can achieve high concentrations in solution (Fig. 3). At the two sites farthest from the trench, by contrast, the concentrations of Ca and Sr are minuscule because these sites have a source of carbonate alkalinity, the high concentrations of which remove Ca and Sr by precipitation of $CaCO_3$. In fact it is likely that solutions from all of these sites are saturated with $CaCO_3$, and that the concentrations of the constituent species are determined by the presence or absence of an external source of carbon. Its presence beneath seamounts 85 to 90 km from the trench indicates that, with increasing depth and temperature, decarbonation or carbonate dissolution has joined dehydration as a major process at the top of the downgoing plate. Although we hypothesize that the upwelling pore waters are saturated with $CaCO_3$ throughout their ascent, this does not mean that $CaCO_3$ will form in large quantities in the serpentinite. Except in the shallow subsurface mixing zone, where seawater is available, its formation will be limited by a shortage of dissolved carbonate at sites near the trench and by a shortage of Ca, in solution and in harzburgite, farther from the trench.

Like alkalinity, dissolved sulfate is also higher farther from the trench, reaching a concentration nearly twice that in seawater at Conical Seamount 90 km distant (Fig. 10). Sulfur is also probably supplied externally, considering its abundance in subducted oceanic crust and its near absence in the serpentinite mud (Table 2), and mobilized as sulfate. Whether its increase with distance from the trench results mainly from a difference in supply, or whether its concentration is simply limited in the high-Ca solutions nearer the trench by gypsum saturation, is not clear. The difference in the extrapolated sulfate concentrations between the two high-Ca sites is large, as are the uncertainties in this extrapolation. Farther from the trench, where the highest sulfate concentrations are found, the near-zero Ca concentrations that result from high carbonate alkalinity make gypsum saturation unlikely.

### 5.3. Inferring Temperature at the Top of the Subducting Plate

Other elements that are depleted in pore water near the trench but enriched farther away are Na (relative to chlorinity), K, Rb, and B. The net transfer of these elements between solids and solution depends on temperature for many substrates, including oceanic crustal basalt and sediments. K and Rb are consistently taken up from seawater into alteration minerals at low temperature but leached into solution at high temperature. Na, K, and Rb are taken up into altered basalt at 63°C at the Baby Bare ridge-flank springs, whereas B is leached (Wheat and Mottl, 2000). Na and K were taken up in laboratory experiments reacting seawater with basalt at 70°C but leached into solution at 150°C (Seyfried and Bischoff, 1979). K and B were also leached from basalt at 200° to 500°C (Mottl and Holland, 1978), Rb at 150° to 351°C, and Cs at 251° to 351°C (James et al., 2003), whereas Na was taken up in rock-dominated experiments (Mottl and Holland, 1978; James et al., 2003) but leached in seawater-dominated experiments (Seyfried and Mottl, 1982). When seawater was reacted with sediment under rock-dominated conditions, K was leached at 51° to 350°C, Rb and Cs were taken up at 51° and 99°C but leached at 150° to 350°C, B was taken up at 51°C but leached at 99° to 350°C, and Na transfer was variable (James et al., 2003). Reaction of sediment with an artificial Na-Ca-Cl solution under rock-dominated conditions at 25° to 347°C produced concentrations above those in seawater at ≥25°C for Cs, ≥63°C for Rb, ≥105°C for B, and >347°C for K; Na decreased at all temperatures (You et al., 1996; You and Gieskes, 2001). Borehole water samples from ODP Hole 504B indicate that Na, K, and Rb are taken up into altered basalt at 80° to 162°C, but the amount of uptake varies with increasing temperature over this range, decreasing for K and increasing for Na (Mottl and Gieskes, 1990; Magenheim et al., 1995). Unfortunately, because of vertical mixing in the deeper part of the borehole, the warmer water samples average the net effect of reaction over 80° to 162°C. These data nonetheless suggest that the crossover temperatures in net transport direction for K and Rb are closer to 150°C than to 80°C. As Rb is a much larger ion than K, its crossover temperature is probably lower than that for K, implying that the K crossover occurs considerably above 80°C. It must be noted that most of the experiments were conducted at pressures of 0.04 to 0.08 GPa compared with pressures at the top of the subducting plate ranging from 0.5 to 0.9 GPa (Fig. 11). The effect of higher pressure is difficult to quantify. More experimental work is needed to determine the actual crossover temperatures during reaction with both basalt and sediments at high pressures.

We conclude that K, Rb, and Cs are leached from both basalt and sediment at ≥150°C, and that they are taken up from seawater into altered solids at <80°C (and probably at higher temperatures, especially for K, up to 150°C). Na behaves similarly to K and Rb except that water/rock ratio plays a role, as would be expected because Na is a major element in both solids and solution. B is leached at temperatures as low as 63°C and generally over the entire temperature range.

At the six sites sampled, Cs is consistently above its seawater concentration (Fig. 8), and it appears to be the element most readily leached (Bebout et al., 1999). Na/Cl, Rb, and B are the next species to rise above their values in seawater with distance from the trench (see values in bold in Table 3), at Pacman Seamount subsummit, 64 km from the trench. The temperature

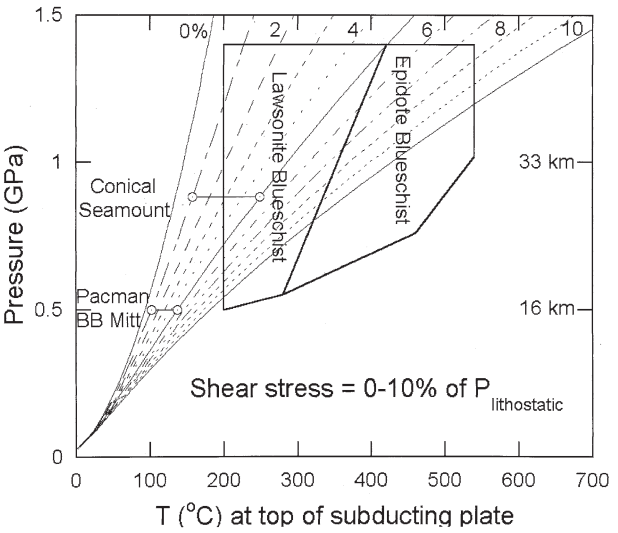


Fig. 11. Temperature at the top of a subducting slab calculated from the analytical expression of Molnar and England (1990; Peacock, 1992) for shear stress of 0%–10% of lithostatic pressure, using parameters appropriate to the Mariana forearc: convergence velocity of 4 cm/yr, subduction dip of 18°, basal heat flux for >80 Ma-old plate of 50 mW/m$^2$, thermal conductivity of 2.5 W/m K, thermal diffusivity of $10^{-6}$ m$^2$/s, density of 3 g/cm$^3$, constants b1 = 1 and b2 = 1.33. For a water depth of 2900 m these pressures correspond to depths of 0 to 50 km below the seafloor, approximately the depth range over which the analytical expression is applicable. Blueschist stability fields are from Peacock (1992). The six sites in this study are bounded by the Baseball (BB) Mitt site on Pacman Seamount and ODP Site 780 on Conical Seamount. Possible temperature ranges are shown for these two sites assuming that shear stress is between 1 and 5% of lithostatic pressure (Peacock, 1996); temperature ranges for all six sites are given in Table 3.

within the oceanic crust at the top of the subducting slab at this site, which we estimate to be ~20 km below the seafloor (Table 3), probably lies between 80° and 150°C. These species are joined by K at Big Blue Seamount, 70 km from the trench, and by sulfate and carbonate alkalinity at South Chamorro Seamount, 85 km from the trench. We have shown that K is relatively unreactive at shallow depths within the serpentinite (see Section 5.1) and that its crossover temperature at depth is probably near 150°C. It is likely, therefore, that the 150°C isotherm within the top of the subducting plate lies approximately beneath Big Blue Seamount, at an estimated depth of ~22 km below the seafloor (Table 3).

The overall intermediate compositions of the upwelling pore waters at the two sites at intermediate distances from the trench, Pacman Seamount subsummit and Big Blue Seamount, are difficult to explain by the model of $CaCO_3$ saturation presented in the previous section. How can these solutions have near-zero concentrations of both Ca and carbonate alkalinity, with only intermediate concentrations of sulfate? We suspect that the short cores and resultant long extrapolations in Figures 3 to 9 have failed us for these two sites. The extrapolated near-zero carbonate alkalinity in Table 3 is more likely to be erroneous than the near-zero Ca concentration; both species are highly reactive in the mixing zone, but carbonate alkalinity would be more quickly driven to zero because Ca is five times more abundant in seawater than is carbonate alkalinity. We believe

that the upwelling pore waters at Pacman Seamount subsummit and Big Blue Seamount are in fact low in Ca and high in carbonate alkalinity, and so resemble the two seamounts farther from the trench rather than the two closer to the trench.

If this is correct, then the temperature at which an external source of carbonate alkalinity becomes available is the same as that at which Na (relative to chlorinity), Rb, and B are first leached from the top of the subducting plate, i.e., between 80° and 150°C. In any case dissolved carbon is supplied abundantly from the source regions beneath South Chamorro and Conical Seamounts, which we estimate to be ~27 to 29 km below the seafloor at temperatures ≥150°C, based on K leaching. Sulfate is also supplied in excess of its seawater concentration at these two sites and so must originate in the same deep source region.

The temperatures inferred from K and Rb in the upwelling pore waters are consistent with the mineral assemblages of blueschist facies metabasite grains suspended in the serpentinite mud recovered from ODP Site 778 on Conical Seamount. Maekawa et al. (1993) inferred that these mafic fragments were metamorphosed at 150° to 250°C and 0.5 to 0.65 GPa, equivalent to depths of 16 to 21 km below seafloor, shallower than the 29 km we have estimated for this site 90 km from the trench (Table 3). Fryer et al. (2000) made a preliminary estimate for metabasite grains in serpentinites dredged from South Chamorro Seamount of <350°C at <0.8 GPa, equivalent to a depth of <26 km, close to our estimate of 27 km. Our temperature estimates are also consistent with a low-temperature serpentine assemblage dominated by lizardite at South Chamorro Seamount summit (Shipboard Scientific Party, 2002) and by chrysotile at Conical Seamount summit (Fryer and Mottl, 1992). Benton (1997) inferred a likely temperature range of serpentinization beneath Conical Seamount of 150° to 200°C based on the oxygen isotopic composition of pore water at ODP Site 780.

Theoretical estimates of temperature in subduction zones are hampered by a lack of constraint on two processes that have potentially large effects: shear heating (Peacock, 1992, 1996) and induced convection in the overlying mantle wedge (Kincaid and Sacks, 1997). Both of these processes depend on how tightly coupled the two plates are across the décollement, which is poorly known. Each can affect the temperature at the top of the subducted plate by as much as several hundred degrees Celsius for a reasonable range of parameters. Convection in the mantle wedge induced by subduction does not affect temperature in the shallow part of a subduction zone, at less than ~50 km depth (Peacock, 1996), where the mantle is brittle rather than ductile. This process can therefore be neglected for the sites we studied, where the estimated depths are 16 to 29 km. In fact it is unlikely that serpentinite mud volcanoes would form above ductile mantle as there would be no fractures through which the serpentinite mud could readily ascend. For shallow depths where induced convection is not important, the effects of shear heating on temperature can be calculated from the analytical expressions of Molnar and England (1990; Peacock, 1992) (Fig. 11). Assuming that shear stress is in the range 1 to 5% of total lithostatic pressure (Peacock, 1996), these expressions yield temperature ranges of 102° to 137°C for the shallowest site, Baseball Mitt on Pacman Seamount (16 km), and 157° to 249°C for the deepest site, Conical Seamount (29 km) (Table 3). The latter range is nearly identical to the 150° to 250°C cited above based on metamorphic mineral assemblages recovered from the same seamount (Maekawa et al., 1993). Unfortunately, the similarity results from circular reasoning, as Peacock (1996) used these mineralogical data to constrain the likely range in shear stress. The ranges are certainly reasonable, however, as the observed transitions in solution composition (Fig. 10) between these two sites, especially the transition from uptake to leaching of K and Rb, probably occur within this temperature range. As discussed above, the range estimated for the source region of waters upwelling from 20 km depth beneath Pacman Seamount subsummit is 80° to 150°C; the range estimated from Figure 11 for this depth is 120° to 170°C for shear stress of 1 to 5% of lithostatic pressure (Table 3). Of course, as noted above, there is a large uncertainty in our estimate for depth to the top of the subducting slab.

These temperatures can be related to conditions required for dehydration and decarbonation. Dehydration is believed to progress more or less continuously with increasing temperature and includes 1) expulsion of interlayer water and conversion of opal-A to opal-CT at 30° to 80°C, 2) expulsion of interlayer water and conversion of smectite to illite at 50° to 150°C, 3) dehydration of sedimentary minerals, mainly clays, at >250°C, and 4) dehydration of hydrous alteration phases in the basaltic oceanic crust at >450°C (Peacock, 1990). These dehydration reactions are accompanied by breakdown of heavier hydrocarbons to methane in subducted sediment at 60° to 150°C (Peacock, 1990). Kerrick and Connolly (1998, 2001a,b) used thermodynamic data to model decarbonation of sedimentary and vein carbonates in ophicarbonates, marine sediments, and altered basalts and found that it did not occur below 400° to >540°C at ~0.8 GPa. Their approach allowed for production of a fluid containing $H_2O$ and $CO_2$ but not for back-reaction of this fluid with the mineral assemblages, so that carbonate dissolution was not considered. It is likely that the decarbonation we have documented between 55 and 85 km from the trench begins at about the same temperature as leaching of K, ~150°C, by reactions between clay minerals and carbonates that liberate $CO_2$. This $CO_2$ forms carbonic acid, which then hydrolyzes silicate minerals to produce the carbonate alkalinity we observed.

## 6. CONCLUSIONS

We have sampled pore waters from ten serpentinite mud volcanoes in the Mariana outer forearc (Table 1) and one in the Izu-Bonin outer forearc, by conventional gravity and piston coring, push coring from the ROV *Jason,* and deep-sea (ODP) drilling. Six sites on five of these seamounts, from 13°47′N to 19°33′N and 52 to 90 km behind the trench axis, yielded upwelling pore waters that had lower chlorinity than bottom seawater. Based on their composition (Table 3 and Fig. 10) we conclude the following about these upwelling pore waters.

Chlorinity varies greatly but not systematically across the outer forearc. $H_2O$ is introduced by dehydration of sediments and altered basalt at the top of the subducting Pacific Plate, estimated to be 16 to 29 km deep for the six sites. Chloride probably comes mainly from pore water that was not squeezed out by compaction, and possibly from seawater introduced at shallow depths. At some sites $^{87}Sr/^{86}Sr$ is enriched relative to the mantle value, probably from the same sources. $H_2O$ is

continuously consumed by serpentinization as the pore waters ascend, causing chlorinity to increase. Variations in these processes produce variable chlorinity from site to site.

Carbonate alkalinity and sulfate are low near the trench and high farther away because, at a depth between 17 and 27 km and a temperature between 80° and 150°C, carbonate dissolution joins dehydration as a major process at the top of the subducting slab. Ca and Sr show the opposite trends because the ascending solutions are uniformly saturated with $CaCO_3$, which limits Ca and Sr to low concentrations at sites farther from the trench where there is an external source of carbonate alkalinity. In the absence of such a source near to the trench, Ca and Sr reach high concentrations by leaching from subducted sediments or basalt at the deep source, or from harzburgite during ascent. Sulfate is likewise supplied from the top of the downgoing plate, but its concentration may be limited at sites near the trench, where Ca and Sr are high, by saturation with gypsum.

Na/Cl, K, Rb, Cs, and B increase away from the trench as temperature increases at the top of the subducting plate. K and Rb are known to be taken up from seawater into alteration minerals at temperatures below ~80°C but are leached into solution at ≥150°C. The transition from uptake of these elements to leaching, relative to their concentrations in seawater, takes place at our sites between 55 and 70 km from the trench, at estimated depths of 17 to 22 km below the seafloor. We estimate that the 150°C isotherm lies approximately beneath Big Blue Seamount at ~22 km depth, where we surmise that carbonate dissolution first becomes important along with dehydration. These temperatures are consistent with independent estimates from metamorphic mineral assemblages in mafic fragments from serpentinite mud from Conical and South Chamorro Seamounts (Maekawa et al., 1993; Fryer et al., 2000) and from the oxygen isotopic composition of pore waters from Conical Seamount (Benton, 1997), as well as with theoretical estimates, which range from 102° to 249°C for our six sites at 52 to 90 km from the trench and 16 to 29 km deep (Table 3 and Fig. 11).

Three sets of data allow us to estimate the effects of reactions that take place at shallow depth beneath the seafloor on mixing of the upwelling pore waters with bottom seawater. Near the trench, where Ca is high and carbonate alkalinity is low, there are large losses from solution, in order of extent, of 1) Ca, as $CaCO_3$ and possibly gypsum and in exchange for Na; 2) Mg, in exchange for Na and as brucite; 3) sulfate, removed either as bisulfide or as gypsum; and 4) alkalinity, as brucite and $CaCO_3$. These losses are balanced by substantial leaching of Na. Farther from the trench, where carbonate alkalinity is high and Ca is low, there are large losses from solution, in order of extent, of 1) sulfate, reduced to bisulfide; 2) Mg, in exchange for Ca and as brucite; and 3) Ca, as $CaCO_3$ and in exchange for Na. These losses are balanced by minor leaching of Na, in exchange for Ca, and production of alkalinity by microbial sulfate reduction. In all three data sets Sr, Ba, Si, and F are lost and K and $^{18}O/^{16}O$ are relatively unreactive.

The composition of these upwelling pore waters thus provides insight into processes and conditions at the top of the subducting Pacific Plate beneath the outer Mariana forearc, some of the first processes that occur within the subduction factory.

*Acknowledgments*—We thank the crews of the R/V *Thomas G. Thompson* of the University of Washington, the R/V *Yokosuka* and *Shinkai-6500* of the Japan Agency for Marine Science and Technology (JAMSTEC), and the ROV *Jason* from Woods Hole Oceanographic Institution, as well as Chris Moser of the Coring Facility at Oregon State University, for able technical assistance. This paper was greatly improved as a result of thorough and thoughtful reviews by Drs. H. Chiba, J. Gieskes, W.E. Seyfried Jr., and M. Kusakabe. This work was funded by NSF-OCE 9633415 (to Fryer, Mottl, and Wheat), 0002584 (to Fryer and Mottl), 0002672 (to Wheat), and the U.S. Science Support Program of the Ocean Drilling Program (to Mottl). This is contribution number 6394 from the School of Ocean and Earth Science and Technology (SOEST) of the University of Hawaii.

*Associate editor:* M. Kusakabe

## REFERENCES

Bebout G. E. (1995) The impact of subduction-zone metamorphism on mantle-ocean chemical cycling. *Chem. Geol.* **126,** 191–218.

Bebout G. E., Ryan J. G., Leeman W. P., and Bebout A. E. (1999) Fractionation of trace elements by subduction-zone metamorphism—Effect of convergent-margin thermal evolution. *Earth. Planet. Sci. Lett.* **171,** 63–81.

Benton L. D. (1997) Origin and evolution of serpentine seamount fluids, Mariana and Izu-Bonin forearcs: Implications for the recycling of subducted material. Ph.D. thesis. University of Tulsa.

Fryer P., Ambos E. L., and Hussong D. M. (1985) Origin and emplacement of Mariana forearc seamounts. *Geology* **13,** 774–777.

Fryer P. and Fryer G. (1987) Origins of nonvolcanic seamounts in a forearc environment. In *Seamount Islands and Atolls* (eds. B. Keating et al.), pp. 61–69. Monograph 43. American Geophys. Union.

Fryer P., Saboda K. L., Johnson L. E., Mackay M. E., Moore G. F., and Stoffers P. (1990) Conical Seamount: SeaMARC II, *Alvin* submersible and seismic reflection studies. *Proc. ODP Init. Repts.* **125,** 69–80.

Fryer P. and Mottl M. J. (1992) Lithology, mineralogy and origin of serpentinite muds recovered from Conical and Torishima forearc seamounts: Results of Leg 125 drilling. *Proc. ODP Sci. Res.* **125,** 343–362.

Fryer P., Pearce J. A., Stokking L. B., et al. (1992) *Proceedings of ODP Sci. Res.* **125**, College Station, TX (Ocean Drilling Program), 716 pp.

Fryer P. and Mottl M. J. (1997) *Shinkai 6500* investigations of a resurgent mud volcano on the southeastern Mariana forearc. *JAMSTEC J. Deep Sea Res.* **13,** 103–114.

Fryer P., Mottl M. J., Johnson L. E., Haggerty J. A., Phipps S. and Maekawa H. (1995) Serpentine bodies in the forearcs of Western Pacific convergent margins: Origin and associated fluids. In *Active Margins and Marginal Basins of the Western Pacific* (eds. B. Taylor and J. Natland), pp. 259–279. Monograph 88. American Geophys. Union.

Fryer P., Wheat C. G., and Mottl M. J. (1999) Mariana blueschist mud volcanism: implications for conditions within the subduction zone. *Geology* **27,** 103–106.

Fryer P., Lockwood J. P., Becker N., Phipps S. and Todd C. S. (2000) Significance of serpentine mud volcanism in convergent margins. In *Ophiolites and Oceanic Crust: New Insights from Field Studies and the Ocean Drilling Program* (eds. Y. Dilek, E. M. Moores, D. Elthon and A. Nicolas), pp. 35–51. Special Paper 349. GSA.

Haggerty J. A. and Chaudhuri S. (1992) Strontium isotopic composition of the interstitial waters from Leg 125: Mariana and Bonin forearcs. *Proc. ODP Sci. Res.* **125,** 397–400.

Hussong D. M. and Fryer P. (1981) Structure and tectonics of the Mariana arc and fore-arc: Drillsite selection surveys. *Init. Repts. Deep Sea Drill. Proj.* **60,** 33–44.

Ishii T., Robinson P. T., Maekawa H., and Fiske R. (1992) Petrological studies of peridotites from diapiric serpentinite seamounts in the Izu-Ogasawara-Mariana forearc, Leg 125. *Proc. ODP Sci. Res.* **125,** 445–485.

James R. H., Allen D. E., and Seyfried W. E. Jr. (2003) An experimental study of alteration of oceanic crust and terrigenous sedi-

ments at moderate temperatures (51 to 350 degrees C): Insights as to chemical processes in near-shore ridge-flank hydrothermal systems. *Geochim. Cosmochim. Acta* **67,** 681–691.

Johnson L. (1992) Mafic clasts in serpentinite seamounts: Petrology and geochemistry of a diverse suite from the outer Mariana forearc. *Proc. ODP Sci. Res.* **125,** 401–413.

Kerrick D. M. and Connolly J. A. D. (1998) Subduction of ophicarbonates and recycling of $CO_2$ and $H_2O$. *Geology* **26,** 375–378.

Kerrick D. M. and Connolly J. A. D. (2001a) Metamorphic devolatilization of subducted marine sediments and the transport of volatiles into the Earth's mantle. *Nature* **411,** 293–296.

Kerrick D. M. and Connolly J. A. D. (2001b) Metamorphic devolatilization of subducted oceanic metabasalts: Implications for seismicity, arc magmatism and volatile recycling, *Earth Planet. Sci. Lett.* **189,** 19–29.

Kincaid C. and Sacks I. S. (1997) Thermal and dynamical evolution of the upper mantle in subduction zones. *J. Geophys. Res.* **102,** 12295–12315.

Lagabrielle Y., Karpoff A.-M., and Cotton J. (1992) Mineralogical and geochemical analyses of sedimentary serpentinites from Conical Seamount. (Hole 778A): Implications for the evolution of serpentine seamounts. *Proc. ODP Sci. Res.* **125,** 325–342.

Maekawa H., Shozui M., Ishii T., Fryer P., and Pearce J. A. (1993) Blueschist metamorphism in an active subduction zone. *Nature* **364,** 520–523.

Magenheim, A. J., Spivack A. J., Alt J. C., Bayhurst G., Chan L.-H., Zuleger E., and Gieskes J. M. (1995) Borehole fluid chemistry in Hole 504B, Leg 137: Formation water or in-situ reaction? *Proc. ODP Sci. Res.* **137/140,** 141–152.

MARGINS Steering Committee. (1998) Program focuses attention on continental margins. *Eos* **79** (11), 137 and 142–143.

Molnar P. and England P. C. (1990) Temperatures, heat flux and frictional stress near major thrust faults. *J. Geophys. Res.* **95,** 4833–4856.

Mottl M. J. (1992) Pore waters from serpentinite seamounts in the Mariana and Izu-Bonin forearcs, Leg 125: Evidence for volatiles from the subducting slab. *Proc. ODP Sci. Res.* **125,** 373–385.

Mottl M. J. and Holland H. D. (1978) Chemical exchange during hydrothermal alteration of basalt by seawater. I. Experimental results for major and minor components of seawater. *Geochim. Cosmochim. Acta* **42,** 1103–1115.

Mottl M. J. and Gieskes J. M. (1990) Chemistry of waters sampled from oceanic basement boreholes, l979-l988. *J. Geophys. Res.* **95,** 9327–9342.

Mottl M. J. and Alt J. C. (1992) Data report: Minor and trace element and sulfur isotopic composition of pore waters from Sites 778 through 786. *Proc. ODP Sci. Res.* **125,** 683–688.

Mottl M. J., Komor S. C., Fryer P., and Moyer C. L. (2003) Deep-slab fluids fuel extremophilic *Archaea* on a Mariana forearc serpentinite mud volcano: Ocean Drilling Program Leg 195. *Geochem. Geophys. Geosyst.* **4** (*11*), 9009. doi: 10.1029/2003 GC000588

Parkhurst D. L. and Appelo C. A. J. (1999) User's guide to PHREEQC–A computer program for speciation, reaction-path, 1D-transport and inverse geochemical calculations. Water-Resources Investigations Report 99-4259. U.S. Geological Survey.

Parkinson I. J., Pearce J. A., Thirlwall M. F., Johnson K. T. M., and Ingram G. (1992) Trace element geochemistry of peridotites from the Izu-Bonin-Mariana forearc, Leg 125. *Proc. ODP Sci. Res.* **125,** 487–506.

Peacock S. M. (1990) Fluid processes in subduction zones. *Science* **248,** 329–337.

Peacock S. M. (1992) Blueschist-facies metamorphism, shear heating and P-T-t paths in subduction shear zones. *J. Geophys. Res.* **97,** 17693–17707.

Peacock S. M. (1996) Thermal and petrologic structure of subduction zones. In *Subduction: Top to Bottom* (eds. D. Scholl, G. Bebout and S. Kirby), pp. 119–133. Monograph 96. American Geophys. Union.

Phipps S. P. and Ballotti D. (1992) Rheology of serpentinite muds in the Mariana-Izu-Bonin forearc. *Proc. ODP Sci. Res.* **125,** 363–372.

Ryan J., Morris J., Bebout G. and Leeman W. (1996) Describing chemical fluxes in subduction zones: Insights from "depth-profiling" studies of arc and forearc rocks. In *Subduction: Top to Bottom* (eds. D. Scholl, G. Bebout and S. Kirby), pp. 263–268. Monograph 96. American Geophys. Union.

Seno T. and Maruyama S. (1984) Paleogeographic reconstruction and origin of the Philippine Sea. *Tectonophysics* **102,** 53–84.

Seyfried W. E. Jr. and Bischoff J. L. (1979) Low temperature basalt alteration by seawater: An experimental study at 70° and 150°C. *Geochim. Cosmochim. Acta* **43,** 1937–1947.

Seyfried W. E. Jr. and Mottl M. J. (1982) Hydrothermal alteration of basalt by seawater under seawater-dominated conditions. *Geochim. Cosmochim. Acta* **46,** 985–1002.

Shipboard Scientific Party. (1990) Site 780. *Proc. ODP Init. Repts.* **125,** 147–178.

Shipboard Scientific Party. (2002) Site 1200. *Proc. ODP Init. Repts.* **195,** 1–173.

Uyeda S. (1982) Subduction zones: An introduction to comparative subductology. *Tectonophysics* **81,** 133–159.

Wheat C. G. and Mottl M. J. (2000) Composition of pore and spring waters from Baby Bare: Global implications of geochemical fluxes from a ridge flank hydrothermal system. *Geochim. Cosmochim. Acta* **64,** 629–642.

You C.-F., Castillo P. R., Gieskes J. M., Chan L. H., and Spivack A. J. (1996) Trace element behavior in hydrothermal experiments: Implications for fluid processes at shallow depths in subduction zones. *Earth Planet. Sci. Lett.* **140,** 41–52.

You C.-F. and J.M. Gieskes. (2001) Hydrothermal alteration of hemipelagic sediments: Experimental evaluation of geochemical processes in shallow subduction zones. *Appl. Geochem.* **16,** 1055–1066.